bone growth. Cell **84** : 911-921, 1996

5) Segev O, Chumakov I, Nevo Z, et al : Restrained chondrocyte proliferation and maturation with abnormal growth plate vascularization and ossification in human FGFR-3 (G380R) transgenic mice. Hum Mol Genet **9** : 249-258, 2000

6) Matsui Y, Yasui N, Kimura T, et al : Genotype phenotype correlation in achondroplasia and hypochondroplasia. J Bone Joint Surg Br **80** : 1052-1056, 1998

7) Thauvin-Robinet C, Faivre L, Lewin P, et al : Hypochondroplasia and stature within normal limits ; another family with an Asn540Ser mutation in the fibroblast growth factor receptor 3 gene. Am J Med Genet A **119** : 81-84, 2003

8) Rousseau F, Bonaventure J, Legeai-Mallet L, et al : Clinical and genetic heterogeneity of hypochondroplasia. J Med Genet **33** : 749-752, 1996

9) The HYP Consortium : A gene (PEX) with homologies to endopeptidases is mutated in patients with X-linked hypophosphatemic rickets. Nat Genet **11** : 130-136, 1995

10) ADHR Consortium : Autosomal dominant hypophosphataemic rickets is associated with mutations in FGF23. Nat Genet **26** : 345-348, 2000

11) Jonsson KB, Zahradnik R, Larsson T, et al : Fibroblast growth factor 23 in oncogenic osteomalacia and X-linked hypophosphatemia. N Engl J Med **348** : 1656-1663, 2003

12) Mornet E : Hypophosphatasia ; the mutations in the tissue-nonspecific alkaline phosphatase gene. Hum Mutat **15** : 309-315, 2000

13) Matsui Y, Kimura T, Tsumaki N, et al : A recurrent 1992delCT mutation of the type X collagen gene in a Japanese patient with Schmid metaphyseal chondrodysplasia. Jpn J Hum Genet **41** : 339-342, 1996

14) Matsui Y, Yasui N, Kawabata H, et al : A novel type X collagen gene mutation (G595R) associated with Schmid-type metaphyseal chondrodysplasia. J Hum Genet **45** : 105-108, 2000

15) Bateman JF, Freddi S, Nattrass G, et al : Tissue-specific RNA surveillance? Nonsense-mediated mRNA decay causes collagen X haploinsufficiency in Schmid metaphyseal chondrodysplasia cartilage. Hum Mol Genet **12** : 217-225, 2003

16) Hall CM : International nosology and classification of constitutional disorders of bone (2001). Am J Med Genet **113** : 65-77, 2002

Increase of smooth muscle cell migration and of intimal hyperplasia in mice lacking the α/β hydrolase domain containing 2 gene

Keishi Miyata [a,b], Yuichi Oike [c], Takayuki Hoshii [a], Hiromitsu Maekawa [c], Hisao Ogawa [b], Toshio Suda [c], Kimi Araki [a], Ken-ichi Yamamura [a,*]

[a] Department of Developmental Genetics, Institute of Molecular Embryology and Genetics, Kumamoto University School of Medicine, 4-24-1 Kuhonji, Kumamoto 862-0976, Japan
[b] Department of Cardiovascular Medicine, Graduate School of Medical Sciences, Kumamoto University, 1-1-1 Honjo, Kumamoto 860-8556, Japan
[c] Department of Cell Differentiation, The Sakaguchi Laboratory, Keio University School of Medicine, Tokyo 160-8582, Japan

Abstract

Multiple steps, including the migration of vascular smooth muscle cells (SMCs), are involved in the pathogenesis of atherosclerosis. To discover genes which are involved in these steps, we screened mutant mouse lines established by the exchangeable gene trap method utilizing X-gal staining during their embryonic development. One of these lines showed strong reporter gene expression in the vitelline vessels of yolk sacs at embryonic day (E) 12.5. The trap vector was inserted into the fifth intron of α/β hydrolase domain containing 2 (Abhd2) gene which was shown to be expressed in vascular and non-vascular SMCs of adult mice. Although homozygous mutant mice were apparently normal, enhanced SMC migration in the explants SMCs culture and marked intimal hyperplasia after cuff placement were observed in homozygous mice in comparison with wild-type mice. Our results show that Abhd2 is involved in SMC migration and neointimal thickening on vascular SMCs.
© 2005 Elsevier Inc. All rights reserved.

Keywords: Gene trap; α/β hydrolase protein; Abhd2; Smooth muscle cell; Migration; Cuff placement model; Neointimal hyperplasia; Atherosclerosis; Alveolar type II cell; Hepatocyte

Smooth muscle-associated protein 8 (smap8), epoxide hydrolase and retinoid-inducible serine carboxypeptidase (RISC), which are members of the α/β hydrolase family, are all reported to be related to vascular smooth muscle cell proliferation and the progression of atherosclerosis [1–3]. In addition, one of these members, epoxide hydrolase, has been found to play an important role in the pathogenesis of atherosclerosis as revealed by a human polymorphism study [4].

The α/β hydrolase fold family consists of hydrolytic enzymes of widely differing phylogenetic origin. Each of these family members has the same protein fold,

termed as the α/β hydrolase fold [5,6]. The core of each enzyme is similar: an α/β-sheet of five to eight β-sheets connected by α-helices to form an α/β/α sandwich. In most of the family members, the β-strands are parallel; some though show an inversion in the order of the first strands, resulting in an antiparallel orientation. These enzymes diverge from a common ancestor so they preserve the arrangement of the catalytic residues, not the binding sites. They all have a nucleophile–histidine–acid catalytic triad, the elements of which are borne on loops which are the best-conserved structural features in the fold. Only the histidine in the catalytic triad is completely conserved, with the nucleophile and acid loops containing more than one type of amino acid. The nucleophile can be a Ser, Cys or Asp residue while the acid loops accommodate an Asp or Glu residue.

* Corresponding author.
E-mail address: yamamura@gpo.kumamoto-u.ac.jp (K. Yamamura).

In mice, three cDNA encoding proteins containing an α/β hydrolase fold were cloned from lung cDNA [7]; they were named as lung α/β hydrolase (Labh) 1, 2, and 3. These are now termed as abhydrolase domain containing (Abhd) 1, 2 or 3. RT-PCR analyses showed that these three genes are widely, but differentially expressed in many tissues. The expression of Abhd1 and Abhd3 was highest in the liver and lowest in the spleen, whereas the expression of Abhd2 was high in the testis and the spleen. The Abhd1 catalytic triad was identified as Ser211, Asp337, and His366. In addition, all three Abhd proteins are shown to have a single predicted amino-terminus transmembrane domain. Although proteins in this family generally act as enzymes such as dienelactone hydrolases, haloalkane dehalogenases, carboxypeptidases, acetylcholinesterases, or lipases, the specific functions of the three Abhd proteins are unknown.

The gene trap strategy using embryonic stem (ES) cells is a powerful method for both the identification of genes and the subsequent establishment of mutant lines [8,9]. We performed gene trap insertional mutagenesis using the trap vector pU-Hachi, and isolated a clone, Ayu8025, in which the trap vector was inserted into the Abhd2 gene. In the present study, we found that Abhd2 deficient mice appear normal without any apparent defect in their vascular development; however, they showed both enhanced SMC migration in the explants SMCs culture and marked intimal hyperplasia after cuff placement, suggesting that Abhd2 in vascular SMCs negatively regulates the formation of neointimal hyperplasia due to vascular injury.

Materials and methods

Generation of gene trap mice. The Ayu8025 gene trap line was isolated as previously described [10]. Chimeric mice were produced by aggregating ES cells with eight-cell embryos. The chimeric male mice were backcrossed to C57BL/6 females to obtain F1 heterozygotes. In this study, we used mice of the F9 generations.

Cloning of genomic DNA and genotyping. Plasmid rescue was performed to obtain flanking genomic DNA as described [10]. DNA samples for genotyping were isolated from the tails of embryos, newborn mice, and adult mice for genotyping. Genotyping was done with PCR using tail genomic DNA as a template. For wild-type alleles, a 5′ primer, G1 (5′-GAGGTCCTCTGCTCCCTGTAT-3′), located in the deleted region by the trapping event, and a 3′ primer, G2 (5′-GTAAGAGCTCCCTTGACTTTCC-3′), located in the sixth exon, were used to generate a 663 bp wild-type fragment. To detect the trap allele, another 5′ primer, G3 (5′-AGCGGATAACAATTTCACAC AGGA-3′), located in the pUC19, and the 3′ primer G2 were used to generate a 425 bp fragment. For PCR analysis, the DNA was subjected to 30 cycles (30 s at 94 °C; 60 s at 59 °C; and, 60 s at 72 °C) using 0.5 U of Taq polymerase (Perkin–Elmer, Foster City, CA).

RNA analysis. Rapid amplification of cDNA ends (RACE) using the 5′ and 3′ RACE system (Invitrogen, Carlsbad, CA) was utilized to characterize the trapped gene, 5′ or 3′, as described previously [11]. Total RNAs were extracted from various tissues and were used for RT-PCR analysis. For Northern blot analysis, 10 μg poly(A)$^+$ RNAs isolated from various tissues were purified with the OligotexTM-dT30

mRNA purification kit (Takara Shuzo, Kyoto, Japan), as described previously [12]. An Abhd2 cDNA probe (nucleotides 52–550) was prepared using DIG-labeled antisense probe riboprobes (Roche, Germany) and used for the Northern blot analysis. Primers used in the RT-PCR include the following: A1 (5′-GTTGGACTGCTGGAGTC AAT-3′) located in the 1st exon (nucleotide number 48–67); A2 (5′-AC TGCTTCTCGCTGTGGTTG-3′) located in the fifth exon (nucleotide number 586–605); B2 (5′-TCCTCTTTGTTAGGGTTCTTC-3′) located in the splice acceptor of the trap vector; C1 (5′-GACATATCCC CAGACCCAGC-3′) located in the sixth exon (nucleotide number 763–782); C2 (5′- ACAGCCGGCTCAAG-3′) located in the eighth exon (nucleotide number 1051–1064); D1 (5′-CGACCCCTTGGTGC ACGAAAG-3′) located in the 10th exon (nucleotide number 1213–1233); and D2 (5′-CCAGGGAGAGCCGCCTACTTG-3′) located in the 11th exon (nucleotide number 1594–1604). Changes in the mRNA levels of Abhd2 in the cuff-injured areas were measured by reverse transcriptase-polymerase chain reaction (RT-PCR). The total RNA was extracted from normal and cuff-injured femoral arteries and RT-PCR was performed using two set primers to generate a 432 bp fragment: 5′-TCGACCTCTTCGAGCCCCTG-3′ located in the fourth exon (nucleotide number 513–532); and 5′-CCTGCGGCACTGGTC-3′ located in the seventh exon (nucleotide number 929–944). Each RNA quantity was normalized to its respective glyceraldehyde-3-phosphate dehydrogenase (GAPDH) mRNA quantity.

In situ hybridization. In situ hybridization analyses were performed on whole mounts and sections of staged embryos as described previously [13] and on adult tissue section samples utilized a VENTANA in situ hybridization machine. DIG-UTP-labeled antisense and control sense probe riboprobes (Roche, Germany) were synthesized by transcription from the pGEM-T vector plasmid with SP6 or T7 on RNA polymerase and then purified on Quick Spin Columns (Bio-Rad, Hercules, CA).

Histochemistry, immunohistochemistry, and β-galactosidase staining. For immunofluorescent detection, tissues were fixed with 4% paraformaldehyde and then washed with three rinses of PBS. Sections were incubated in 4% normal goat serum at room temperature for 1 h followed by 12–15 h in a primary antibody solution of PBS/Triton. The α-SMA immunoreactivity was detected by an α-SMA/HRP monoclonal antibody (Dako, Carpinteria, CA) diluted 1:500, followed by anti-rat biotin-labeled second antibodies at a 1:500 dilution. The β-galactosidase staining for sample was performed as described [14].

Preparation of explants, proliferation, and migration assay. Mice aorta explant cultures were performed as described [15]. Thoracic aortas of adult mice (age 10–12 weeks, wild-type, and homozygote mice) were dissected and the endothelium and periadvential fat was removed by gentle abrasion. Then, the aortas were cut into 2 × 2 mm explants. The explants were individually plated with the lumen side down into collagen type I-coated 12-well multiplates and cultured in 150 μL Dulbecco's modified Eagle's medium (DMEM) containing 10% fetal bovine serum, penicillin/streptomycin, and 2-mercaptoethanol. To characterize the cells migrating from explants, cells were fixed and stained for SM α-actin. For the experiments, SMCs in a subconfluent state at the third and fifth passage were used.

For the proliferation assay, SMCs were plated on collagen type I-coated 96-well plates (5 × 10³ cells/well) and then incubated with DMEM containing 0.3% BSA and PDGF-BB (10 ng/mL) (PeproTech EC, UK) for 3 days. Cell numbers per well were counted with the use of the Cell Counting Kit-8 (Dojindo, Kumamoto, Japan).

The migration assay was performed with Transwell (Corning, Nagog, MA) 24-well tissue culture plates composed of an 8 μm pore polycarbonate membrane. The inner chamber membrane was coated with 0.1% gelatin. SMCs were then seeded on the inner chamber of the Transwell at a concentration of 5 × 10³ cells/100 μL. The inner chamber was placed into the outer chamber containing recombinant human PDGF-BB (10 ng/mL), and then incubated for 6 h at 37 °C. The cells that migrated onto the outer side of the membrane were fixed and stained. The number of migrated cells was counted in the five ran-

domly chosen fields of the duplicated chambers at a magnification of 200× for each sample.

Cuff-induced intimal thickening of the murine femoral artery. The cuff placement surgery was performed according to a method and the sections were stained and measured as described [16]. After the experimental period, the mice were euthanized, and their arterial tissues were fixed in 10% formalin and then embedded in paraffin. The middle segment of the artery was cut into five subserial cross-sections at intervals of 200 μm. The sections were stained using elastica van Gieson or hematoxylin and eosin staining. The areas of the neointima, media, and adventitia were measured utilizing image-analyzing software (NIH Image). To evaluate DNA synthesis, bromodeoxyurine (BrdU, Sigma–Aldrich, St. Louis, MO) was injected at doses of 100 mg/kg SC and 30 mg/kg IP 18 h before euthanasia and then at a dose of 30 mg/kg IP 12 h before euthanasia. Immunohistochemistry using anti-BrdU antibody (Dako, Carpinteria, CA) in serial sections was performed and BrdU index (the ratio of BrdU-positive nuclei versus total nuclei) was calculated.

Statistical analysis. Values are given as means ± SEM. All comparisons were done using the Student's t test for comparisons between groups. $P < 0.05$ is considered significant, and $P < 0.01$ was considered highly significant.

Results

Establishment of Ayu8025 line and identification of trapped gene

We isolated gene trap ES clones using the trap vector pU-Hachi and established 36 mouse trap mouse lines through the production of germline chimeras. We screened these mice by whole mount X-gal staining using embryonic days (E) 12.5 embryos. Interestingly, one of these lines, Ayu8025, showed strong expression of *lacZ* in blood vessels such as vitelline vessels (Fig. 1A) and thus this was further investigated. This mutant mouse line was designated as B6; CB-Abhd2^{GtAyu8025IMEG}. To identify the gene trapped and characterize the insertion site of the trap vector, we performed 5' RACE and plasmid rescues. The trap vector was inserted into the fifth intron of the *Abhd2*

gene. We confirmed that the integration of the trap vector resulted in the deletion of 634 bp of genomic DNA located at nucleotide positions between 63,583 and 64,216 (Fig. 1B). In addition, 2 or 14 bp were deleted from the 5' end or the 3' end of the trap vector, respectively. A tail DNA was used for genotyping by PCR. For the wild-type allele, the G1 primer and the G2 primer were used to generate a 663 bp wild-type fragment. To detect the trap allele, the G3 primer and the G2 primer were used to generate a 425 bp fragment. Using these primers, the genotype of the offspring from the heterozygous inter-cross was easily identified (Fig. 1C). Heterozygous and homozygous mice appeared normal and were fertile. Even at the nineth backcross generation to C57BL/6, 46 homozygous, 114 heterozygous, and 48 wild-type mice were generated among 208 live-born offspring by mating between heterozygote parents. This ratio was consistent with the expected Mendelian distribution.

Northern blot and RT-PCR analyses

In order to examine the tissue specific expression and presence of fusion transcripts, the Northern blot analyses using various adult tissues, including brains, hearts, lungs, livers, spleens, skeletal muscles, kidneys, testes, uteruses, and aortas of wild-type, heterozygous and homozygous mice were performed using a fragment of the *Abhd2* cDNA as a probe. In wild-type mice, 6.8 kb transcripts were detected in all tissues examined except for skeletal muscle (Fig. 2A), although the level of expression was variable among these tissues. This 6.8 kb transcript consists of 1.6 kb of *Abhd2* ORF and 5.2 kb of the 3' UTR region as confirmed by analysis of 3' RACE products. In heterozygous mice, two bands of 6.8 and 5.2 kb were detected (Fig. 2A). In homozygous mutant mice, the 5.2 kb transcripts were detected in the same tissues (Fig. 2A) as in the wild-type mice.
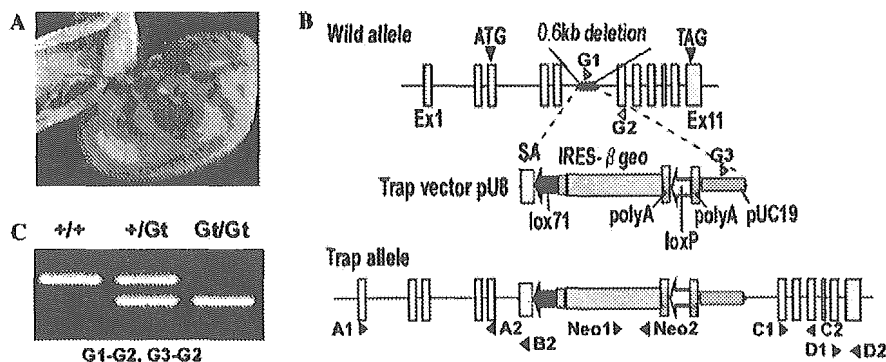

Fig. 1. Insertional mutation of *Abhd2* gene. (A) Expression of *lacZ* at E12.5. X-gal is positive for vitelline vessels in the yolk sac and other tissues including somites. (B) Structure of the wild-type and trap alleles. The trap vector, pU8, was inserted into the fifth intron of the *Abhd2* gene, resulting in a loss of 0.6 kb intronic sequences. The red arrowheads, G1, G2, and G3, are used for the genotyping of mice. Black arrowheads, A1, A2, B2, C1, C2, D1, D2, Neo1, and Neo2, are used for RT-PCR. (C) PCR genotyping. The wild-type or trap allele is detected using G1 and G2 or G1 and G3 primer sets, respectively. +/+, wild-type mouse; +/Gt, heterozygous mouse; Gt/Gt, homozygous mutant mouse.
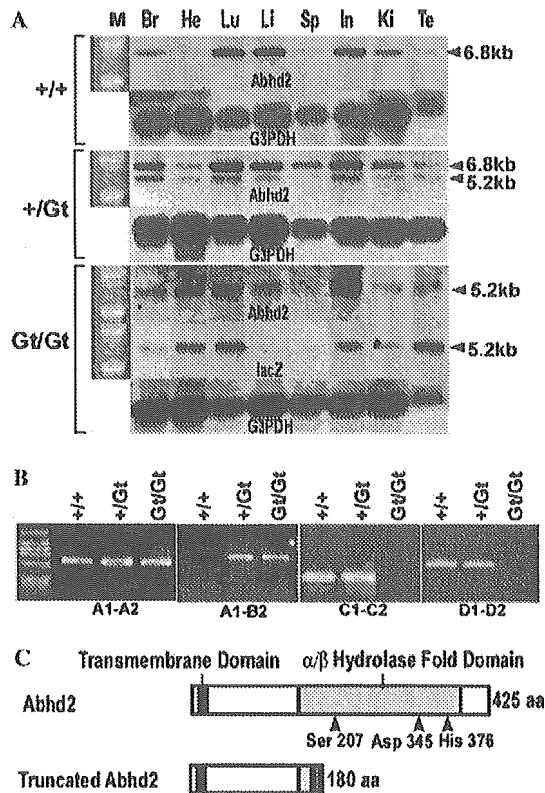
Fig. 2. Disruption of *Abhd2* expression in mutant mice. (A) Northern blot analyses of wild-type (+/+), heterozygous (+/Gt), and homozygous mutant (Gt/Gt) mice. In the +/+ mouse, only a 6.8 kb band was detected in various tissues. In the +/Gt mouse, both 6.8 and 5.2 kb bands were detected. In the Gt/Gt mouse, only a 5.2 kb band which was hybridized with both *Abhd2* and *lacZ* probes was detected. These result suggest that the insertion of trap vector results in the complete loss of wild-type mRNA and in the production of 5.2 kb fusion mRNA. (B) RT-PCR analyses using primers shown in Fig. 1B. Using probes A1 and A2, 558 bp products were detected in +/+, +/Gt, and Gt/Gt mice. Using probes A1 and B2, 724 bp products were only detected in mice carrying the trap allele. When probes C1 and C2 or D1 and D2 were used, 302 or 392 bp products were detected, respectively, in +/+ and +/Gt mice, but not in Gt/Gt mouse. These results suggest that no other alternative splicing occurs in either the wild-type or the trap allele. (C) Schematic diagram of wild-type and truncated *Abhd2* protein. Truncated *Abhd2* protein lacks most of α/β hydrolase fold domain. Arrowheads indicate triad catalytic domains (Ser207, Asp345, and His376). M, size marker; Br, brain; He, heart; Lu, lung; Li, liver; Sp, spleen; In, intestine; Ki, kidney; Te, testis.

The 5.2 kb transcripts were also hybridized with the *lacZ* probe (Fig. 2A), suggesting that this transcript is a fusion message comprised of 0.5 kb truncated *Abhd2* and 4.7 kb *β-geo* mRNA. This was confirmed by sequencing the 5' RACE product.

To examine whether any other alternative splicing product was present or not, RT-PCR analyses were done using probes as described in Materials and methods. Using probes A1 and A2, 558 bp products were detected in wild-type, heterozygous, and homozygous mice (Fig. 2B). As expected, 724 bp products were only de-

tected in mice carrying the trap alleles when probes A1 and B2 were used (Fig. 2B). When probes C1 and C2 or D1 and D2 were used, 302 or 392 bp products were detected, respectively, in wild-type and heterozygous mice (Fig. 2B). These results suggest that no other alternative splicing occurs in either the wild-type or trap allele. Thus, the insertion of a trap vector into the fifth intron results in the complete loss of the wild-type message and in the transcription of a fusion message. As the fusion message contains up to the fifth exon, it was expected to produce a truncated Abhd2 protein that contains only 180 amino acids of N-terminus, but not the catalytic domain of α/β hydrolase fold protein (Fig. 2C).

Analysis of X-gal staining

To analyze cell-type specific expression of the *Abhd2* gene, we performed X-gal staining using tissue sections of adult mice. It is noteworthy that β-galactosidase activity was detected in vascular SMCs, non-vascular SMCs, and the heart, but not in the skeletal muscle cells. Vascular SMCs include those in the aorta (Fig. 3A), small arteries in the skin (arrow in Fig. 3B), arterioles in the ear (arrow in Fig. 3C), and in superior and inferior vena (Fig. 3D). The *lacZ* expression was not detected in veins (arrowhead in Figs. 3B and C), probably because of absence of SMCs. *lacZ* was also expressed in the myocardium of the atrium and ventricles of the heart (Fig. 3E) and in the non-vascular smooth muscle cells such as the bronchial SMC layers (Fig. 3F), uterine SMCs (Fig. 3G), intestinal SMC layers (Fig. 3K), and bladder SMCs (data not shown); however, *lacZ* was not detected in the skeletal muscle cells (Fig. 3H). We confirmed that X-gal positive cells were indeed vascular or non-vascular SMCs, but not endothelial cells, utilizing immuno-histochemical staining with anti-α-smooth muscle actin antibodies (Figs. 3I, J, K, and L). In situ hybridization experiments using the same 5' probe as used for the Northern blot analysis (see Fig. 1) revealed that X-gal positive cells were coincident with those cells that expressed the mouse *Abhd2* mRNA (data not shown), suggesting that *lacZ* staining reflects the expression pattern of the *Abhd2* gene.

X-gal positive cells were also detected in other types of cells, such as hepatocytes around hepatic interlobular areas of liver tissue (Fig. 3M), alveolar type II cells of lung tissue (Fig. 3N), splenic cords (reticular cells) around white pulp in the spleen (Fig. 3O), the cortex area of adrenal gland (Fig. 3P) and other tissues such as islet cells of Langerhans of the pancreas or columnar epithelium cells in ductus deferens (data not shown). In the brain, X-gal was positive in epithelium cells of choroids, granular cells of gyrus dentatus, and external and internal granular cells of the cerebral cortex (data not shown).
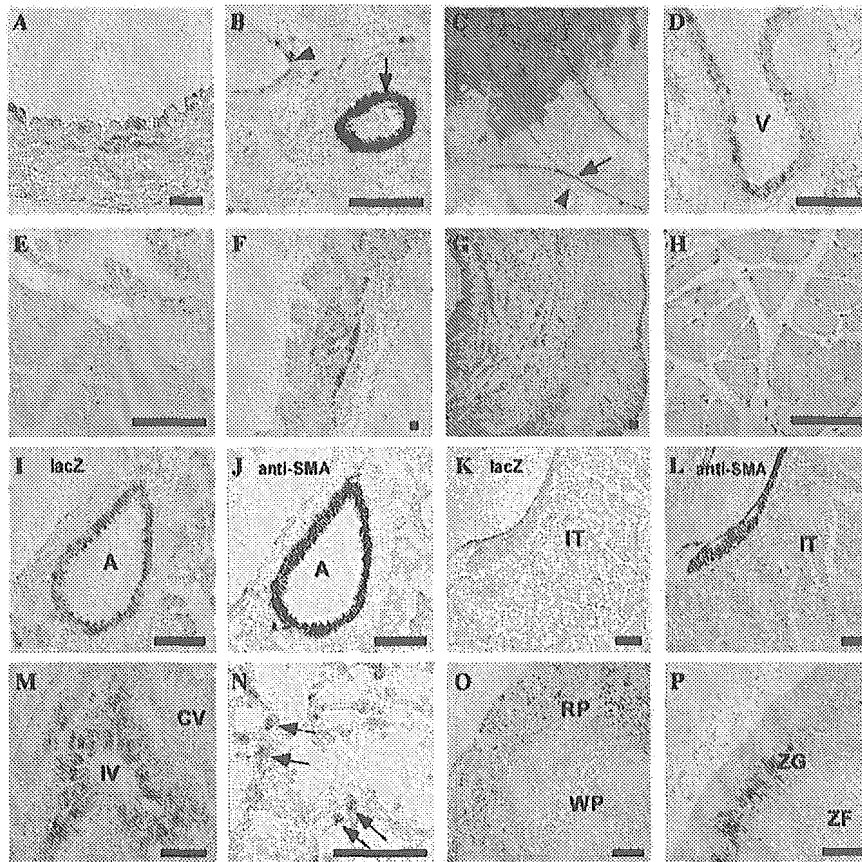
Fig. 3. X-gal staining in heterozygous mice. LacZ expression was detected in vascular SMCs of the aorta (A), small arteries in the skin (arrow in B), arterioles in the ear (C), superior and inferior vena (D), but not in veins (arrowheads in B and C). LacZ was also expressed in the myocardium of the atrium and in the ventricle of the heart (E) and non-vascular smooth muscle cells, such as the bronchial SMC layer (F), uterine SMCs (G), and intestinal SMC layer (K); however, lacZ was not detected in skeletal muscle cells (H). X-gal positive cells are clearly stained with anti-α-smooth muscle actin antibody in both vascular (I, J) or non-vascular tissues (K, L). X-gal positive cells were also detected in other types of cells, such as the hepatocytes around hepatic interlobular area of liver tissue (M), alveolar type II cells of lung tissue (arrows in N), splenic cords (reticular cells) around white pulp in the spleen (O), and the cortex area of the adrenal gland (P). A, artery; V, vein; IT, intestinal tract; IV, interlobular vein; CV, central vein; RP, red pulp; WP, white pulp; ZG, zona glomerulosa; ZF, zona fasciculata. Scale bar = 100 μm
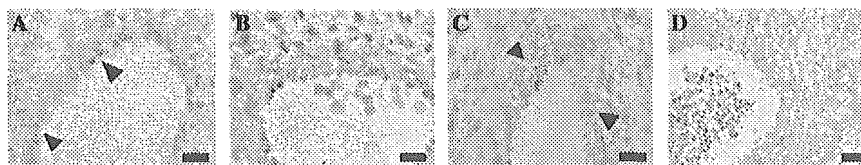

Fig. 4. Developmental expression of lacZ in the aorta. At E10.5, lacZ was expressed in endothelial cells of the dorsal aorta, but not in SMCs (A) At E11.5, lacZ expression was detected in both endothelial cells and in SMCs (B) At E13.5, lacZ was expressed in most of the SMCs (C) At E16.5, lacZ was expressed in all SMCs, but in only a few endothelial cells (D). Thus, the expression of Abhd2 starts in endothelial cells, and then shifts to SMCs during embryonic development. Arrowheads indicate the lacZ positive cells. Scale bar = 25 μm.

Developmental expression of LacZ

As the most characteristic feature of the Abhd2 is its expression in vascular smooth muscle cells, we examined the developmental expression of Abhd2 utilizing X-gal staining on heterozygous embryos. At embryonic day 9.5 (E9.5), weak β-galactosidase expression was detected in the heart. At E10.5 lacZ was expressed in the endothelial cells of the dorsal aorta (Fig. 4A), but not in SMCs. This lacZ expression in the endothelial cells disappeared by E12.5. In contrast, lacZ expression was first detected in SMCs at E11.5 (Fig. 4B). At E13.5, lacZ was being expressed in most of SMCs (Fig. 4C). By E16.5, lacZ was expressed in all SMCs (Fig. 4D). Thus, Abhd2 starts

to be expressed in the endothelial cells, and then its expression shifts into SMCs during E10.5–E13.5.

Function of Abhd2 in vitro and in vivo

Although X-gal staining revealed specific expression of *Abhd2* in vascular SMCs, homozygous mutant mice did not show any over phenotype. Thus, we investigated the role of *Abhd2* on the migration and proliferation of vascular SMCs. To investigate the ability of PDGF-BB-directed SMCs to migrate across Transwell filters, an ex-

plant culture method using mouse SMCs derived from either wild-type or homozygous mutant mice was used. We found that the number of cells that passed through the filters in the presence of gradient of chemo-attractant in homozygotes was 140 ± 22.3 SMCs/field which was significantly higher than the 78.8 ± 17.7 SMCs/field in wild-type mice ($P < 0.05$; (Fig. 5A)).

In the proliferation assay, there was no difference in the PDGF-BB-induced proliferative response of cultured SMCs derived from either wild-type or homozygote (Fig. 5B). These data suggest that *Abhd2* is
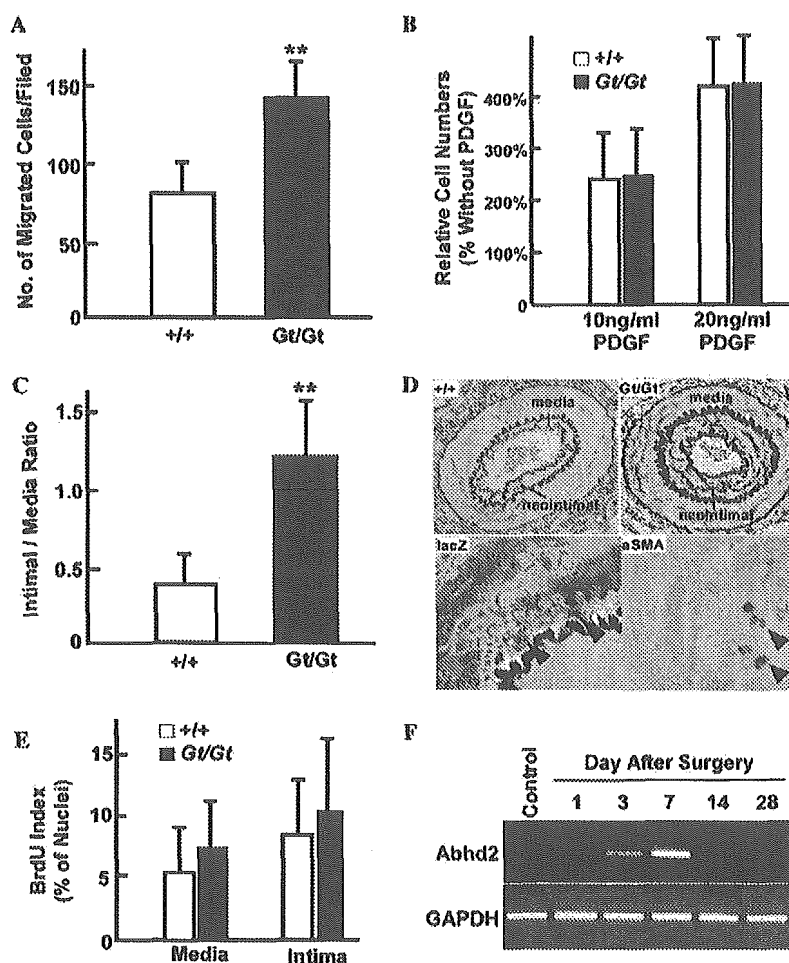

Fig. 5. Function of *Abhd2* in vitro and in vivo. Cultured SMCs derived from the aortas of wild-type and *Abhd2* deficient mice were used for experiments. (A) Transwell assay for SMC migration in the presence of PDGF-BB. The number of cells that passed through the filters in the presence of PDGF-BB (10 ng/mL) in homozygous (Gt/Gt) mice was 140 ± 22.3 SMCs/field which was significantly higher than 78.8 ± 17.7 SMCs/field in the wild-type (+/+) mice ($P < 0.05$). (B) Proliferative ability of SMCs from wild-type or homozygous mice. Data are expressed as a percentage of the cell number in SMCs incubated with culture medium without PDGF-BB. There was no difference in the PDGF-BB-induced proliferative response of cultured SMCs derived from wild-type or homozygous mice. (C) The intimal/media ratio at 28 days after cuff placement. Intimal/media ratio was significantly larger in homozygous mice than in wild-type mice. (D) Sections of the femoral arteries 28 days after cuff placement of wild-type and homozygous mice stained with elastica van Gieson, X-gal, and anti-αSMA antibody. Neointimal thickening was significantly larger in homozygous mice than in wild-type mice, while the adventitial region was similar between them. Cells in the neointimal area expressing *lacZ* (blue) and α smooth muscle actin (blue) are indicated by arrowheads. (E) BrdU uptakes in both the intimal and the medial layers. BrdU uptakes in both intimal and medial layers were not different between the wild-type and homozygote mice. (F) Time course of *Abhd2* mRNA expression after cuff placement. Expression of *Abhd2* increased and reached a maximum level at 7 days and then decreased to an undetectable level by 14 days after cuff placement of the femoral artery. Glyceraldehyde-3-phosphate dehydrogenase (GAPDH) was used as an internal control. Quantitative analysis of the area of explant culture and intimal/media was performed with the NIH Image software. Results represent means $\pm$ SEM of eight experiments. $**P < 0.01$e.

involved in the regulation of SMC migration in response to exogenous factors; therefore, we investigated the in vivo role of *Abhd2* on vascular smooth muscles using the cuff placement model. To examine the effect of cuff placement on the neointimal formation, we analyzed histological sections. In the sham-operated side, no neointimal thickening was found at 7 days or 28 days after surgery in either wild-type or homozygous mice. In the cuff placement side, no neointimal hyperplasia was found at 7 days after surgery in either wild-type or homozygote mice; however, at 28 days after surgery, neointimal hyperplasia was observed in both wild-type and homozygote mice. Neointimal thickening was significantly larger in homozygous mice than in wild-type mice, while the adventitial region was similar between them (Figs. 5C and D). Cells in the neointimal area expressed *lacZ* and α smooth muscle actin (Fig. 5D).

To analyze the proliferative activity of SMCs, DNA synthesis was examined by BrdU uptake 7 days after cuff injury. BrdU uptakes in both intimal and medial layers were not different between the wild-type or homozygote mice (Fig. 5E). Taken together, neointimal hyperplasia in homozygous mice might be caused by the migration of SMCs, but not by the proliferation of SMCs. If the absence of the *Abhd2* expression is involved in enhanced migration of SMCs, the expression of *Abhd2* should be increased after cuff placement in wild-type mice. Thus, we analyzed the time course of *Abhd2* mRNA expression after cuff injury. RT-PCR analysis showed that expression of *Abhd2* increased and reached a maximum level at 7 days after cuff injury of the femoral artery (Fig. 5F). These data indicated that the loss of *Abhd2* resulted in the enhancement of vascular SMCs migration, leading to the neointimal hyperplasia.

Discussion

We have established the Ayu8025 trap mutant line in which the trap vector was inserted into the fifth intron of the *Abhd2* gene, which is one of the α/β hydrolase protein family. This insertion results in the production of fusion transcript which can produce truncated proteins containing 180 amino acids, but lacking triad catalytic triad domains (Ser207, Asp345, and His376) of the *Abhd2* protein. Thus, truncated *Abhd2* protein may lose its function; however, *Abhd2* deficient mice have no obvious phenotype under normal conditions. The ESTHER, the database of the α/β hydrolase fold superfamily of proteins, reported that mouse *Abhd2* protein belongs to the upf_0017subfamily of the α/β hydrolase fold family including mouse *Abhd1* and *Abhd3* [17]. The NCBI database just reported the data on mouse *Abhd4* and *Abhd6*. Further study to examine the cell-type specific expression of these family genes will be re-

quired to assess the possibility that these genes can compensate for a deficiency of *Abhd2*.

From our findings on *Abhd2* expression in vascular SMCs, we performed two experiments to study the function of the *Abhd2* gene. First, the in vitro study demonstrated that the migratory ability of cultured SMCs from *Abhd2* deficient mice was higher than that of wild-type mice. The proliferation ability showed no significant difference between them. This indicates that *Abhd2* plays a critical role for regulating SMC migration. Second, we investigated the role of *Abhd2* in vivo, using the cuff placement model in the mouse femoral artery. *Abhd2* deficient mice showed a marked increase in neointimal area in comparison with that of wild-type mice. On the other hand, there was no difference in the PDGF-BB-induced proliferative response of cultured SMCs derived from either wild-type or homozygote in terms of BrdU labeling in either the intimal or the media region. These results suggest that increased SMC migratory activity is the main cause for the increase of intimal hyperplasia in *Abhd2* deficient mice. However, other growth factors or molecules such as hyaluronic acid, heparin or aminoglycan chains of heparan sulfate proteoglycans, are also reported to affect SMC's migration and proliferation after vascular injury. For example, SMCs secrete a hyaluronic acid into extracellular matrix and hyaluronic acid was involved vascular injury model [18]. Papakonstantinou et al. [19,20] reported that hyaluronic acid plays a role of positive regulator on the PDGF-BB induced SMC proliferation. To investigate the roles of these molecules and the extracellular matrix, further studies using our mouse line will be required.

The mechanisms of intima formation after the cuff placement model are not known yet. Previous studies have shown that medial SMCs are modified and migrate into the intima, where they proliferate and secrete extracellular matrix components [21], and that adventitial fibroblasts migrate into the neointima and differentiate into SMC-like cells [22]. Recently, Tanaka et al. [23] reported that in the cuff placement model bone marrow-derived cells are seldom detected in the neointima, whereas many inflammatory cells in the adventitia are derived from bone marrow cells. Yang et al. also found that the neointimal formation was caused by an interaction and differentiation between macrophages and SMCs in the adventitia area [24]. From these studies, it is not certain that neointimal cells, which express *Abhd2*, migrate from adult bone marrow containing multipotent cells.

Several α/β hydrolase protein family relations to atherosclerosis have been reported. N-myc downstream regulated gene 4 (Ndrg4), also known as smooth muscle-associated protein 8 (smap8) belongs to the α/β hydrolase protein family as predicted from nucleotide sequences. Nishimoto et al. demonstrated that *Ndrg4* expression in vascular SMCs is highly induced by homo-

cysteine. Homocysteine, a sulfur-containing amino acid, is an intermediate metabolite of methionine and is widely recognized as an independent risk factor for atherogenesis [1,25], because patients with severe homocysteinemia suffer from arterial and venous thromboembolic events at an early age. Although overexpression of *Ndrg4* decreased the proliferation and migration of rat aortic smooth muscle cells (A10 cells), PDGF-induced proliferation was significantly enhanced in *Ndrg4* expressed cells. These results suggest that *Ndrg4* is involved in the regulation of mitogenic signaling in vascular SMCs, possibly in response to a homocysteine-induced injury. Soluble epoxide hydrolase (sEH, previously called cytosolic epoxide hydrolase) plays a role in the xenobiotic metabolism and its substrate is epoxyeicosatrienoic acids (EETs), which are synthesized by endothelial cells, and taken up by vascular SMCs. EETs control vascular tone and contribute to pathogenesis of atherosclerosis. sEH is critical in the control of EET levels and inhibitors of sEH have been reported to attenuate vascular SMC proliferation [2,26–28]; furthermore, the human polymorphism of sEH has been reported to be associated with atherosclerosis [4]. Chen et al. cloned retinoid-inducible serine carboxypeptidase (RISC) from vascular SMCs as a target molecule by retinoids. Retinoids are involved in the vascular response to injury and blocks SMC proliferation and attenuates neointimal hyperplasia formation after injury [29]. Taken together, these studies suggest that these α/β hydrolase proteins influence the behavior of vascular SMC and therefore cause vascular disease.

Interestingly, *Abhd2* is expressed in alveolar type II cells of the lung and hepatocytes around the interlobular area of the liver. *Abhd* family genes were identified in a gene screen of human emphysematous tissue [7]. This suggests that *Abhd2* is related to lung homeostasis. Actually, microsomal epoxide hydrolase, one of α/β hydrolase protein family, was expressed in the alveolar epithelial cells including alveolar type II cells [30] and is associated with the genetic susceptibility for the development of emphysematous changes of the lung [31]. In addition, abnormalities in the surfactant homeostasis of alveolar type II cells are shown to cause the emphysematous change [32]. Our result suggests that *Abhd2* in alveolar type II cells protects alveolar tissues from progressive emphysema, however adult *Abhd2* deficient mice showed no significant structural change in lung tissue. The hepatocytes in the liver are quite heterogeneous in terms of the blood supply. Hepatocytes located in the interlobular zone differ from those in the centrilobular zone. In general, the capacity for oxidative energy metabolism, involved in cell protection, is higher in the interlobular zone and xenobiotic metabolism is higher in the centrilobular zone [33,34]. *Abhd2* was expressed more strongly around portal veins at the interlobular zone, suggesting that *Abhd2* at the interlobular zone

protects hepatocytes against exogenous stress factors. Further investigation, such as smoke inhalation experiments or drug administration, may clarify the function of *Abhd2* in the lung or liver.

In conclusion, we find that *Abhd2* contributes to the migration of vascular SMC in the pathologic condition, indicating that *Abhd2* plays an important role in stress response due to external stimulation. Identification of substrates for *Abhd2* will provide an important clue for elucidating the molecular mechanisms of *Abhd2* functioning.

Acknowledgments

References

[1] S. Nishimoto, J. Tawara, H. Toyoda, K. Kitamura, T. Komurasaki, A novel homocysteine-responsive gene, smap8, modulates mitogenesis in rat vascular smooth muscle cells, Eur. J. Biochem. 270 (2003) 2521–2531.

[2] B.B. Davis, D.A. Thompson, L.L. Howard, C. Morisseau, B.D. Hammock, R.H. Weiss, Inhibitors of soluble epoxide hydrolase attenuate vascular smooth muscle cell proliferation, Proc. Natl. Acad. Sci. USA 99 (2002) 2222–2227.

[3] J. Chen, J.W. Streb, K.M. Maltby, C.M. Kitchen, J.M. Miano, Cloning of a novel retinoid-inducible serine carboxypeptidase from vascular smooth muscle cells, J. Biol. Chem. 276 (2001) 34175–34181.

[4] M. Fornage, E. Boerwinkle, P.A. Doris, D. Jacobs, K. Liu, N.D. Wong, Polymorphism of the soluble epoxide hydrolase is associated with coronary artery calcification in African-American subjects: The Coronary Artery Risk Development in Young Adults (CARDIA) study, Circulation 109 (2004) 335–339.

[5] D.L. Ollis, E. Cheah, M. Cygler, B. Dijkstra, F. Frolow, S.M. Franken, M. Harel, S.J. Remington, I. Silman, J. Schrag, et al., The α/β hydrolase fold, Protein Eng. 5 (1992) 197–211.

[6] M. Holmquist, α/β-hydrolase fold enzymes: Structures, functions, and mechanisms, Curr. Protein Pept. Sci. 1 (2000) 209–235.

[7] A.J. Edgar, J.M. Polak, Cloning and tissue distribution of three murine α/β hydrolase fold protein cDNAs, Biochem. Biophys. Res. Commun. 292 (2002) 617–625.

[8] M.J. Evans, M.B. Carlton, A.P. Russ, Gene trapping and functional genomics, Trends Genet. 13 (1997) 370–374.

[9] A. Gossler, A.L. Joyner, J. Rossant, W.C. Skarnes, Mouse embryonic stem cells and reporter constructs to detect developmentally regulated genes, Science 244 (1989) 463–465.

[10] K. Araki, T. Imaizumi, T. Sekimoto, K. Yoshinobu, J. Yoshimuta, M. Akizuki, K. Miura, M. Araki, K. Yamamura, Exchangeable gene trap using the Cre/mutated lox system, Cell. Mol. Biol. (Noisy-le-grand) 45 (1999) 737–750.

[11] Y. Oike, N. Takakura, A. Hata, T. Kaname, M. Akizuki, Y. Yamaguchi, H. Yasue, K. Araki, K. Yamamura, T. Suda, Mice homozygous for a truncated form of CREB-binding protein exhibit defects in hematopoiesis and vasculo-angiogenesis, Blood 93 (1999) 2771–2779.

[12] T. Imaizumi, K. Araki, K. Miura, M. Araki, M. Suzuki, H. Terasaki, K. Yamamura, Mutant mice lacking Crk-II caused by the gene trap insertional mutagenesis: Crk-II is not essential for embryonic development, Biochem. Biophys. Res. Commun. 266 (1999) 569–574.

[13] Y. Kawazoe, T. Sekimoto, M. Araki, K. Takagi, K. Araki, K. Yamamura, Region-specific gastrointestinal Hox code during murine embryonal gut development, Dev. Growth Differ. 44 (2002) 77–84.

[14] Y. Yamauchi, K. Abe, A. Mantani, Y. Hitoshi, M. Suzuki, F. Osuzu, S. Kuratani, K. Yamamura, A novel transgenic technique that allows specific marking of the neural crest cell lineage in mice, Dev. Biol. 212 (1999) 191–203.

[15] M. Kuzuya, A. Iguchi, Role of matrix metalloproteinases in vascular remodeling, J. Atheroscler. Thromb. 10 (2003) 275–282.

[16] Y. Imai, T. Shindo, K. Maemura, M. Sata, Y. Saito, Y. Kurihara, M. Akishita, J. Osuga, S. Ishibashi, K. Tobe, H. Morita, Y. Ohhashi, T. Suzuki, H. Maekawa, K. Kangawa, N. Minamino, Y. Yazaki, R. Nagai, H. Kurihara, Resistance to neointimal hyperplasia and fatty streak formation in mice with adrenomedullin overexpression, Arterioscler. Thromb. Vasc. Biol. 22 (2002) 1310–1315.

[17] T. Hotelier, L. Renault, X. Cousin, V. Negre, P. Marchot, A. Chatonnet, ESTHER, the database of the α/β-hydrolase fold superfamily of proteins, Nucleic Acids Res. 32 (2004) D145–D147 (Database issue).

[18] R.C. Savani, C. Wang, B. Yang, S. Zhang, M.G. Kinsella, T.N. Wight, R. Stern, D.M. Nance, E.A. Turley, Migration of bovine aortic smooth muscle cells after wounding injury. The role of hyaluronan and RHAMM, J. Clin. Invest. 95 (1995) 1158–1168.

[19] E. Papakonstantinou, G. Karakiulakis, M. Roth, L.H. Block, Platelet-derived growth factor stimulates the secretion of hyaluronic acid by proliferating human vascular smooth muscle cells, Proc. Natl. Acad. Sci. USA 92 (1995) 9881–9885.

[20] E. Papakonstantinou, M. Roth, L.H. Block, V. Mirtsou-Fidani, P. Argiriadis, G. Karakiulakis, The differential distribution of hyaluronic acid in the layers of human atheromatic aortas is associated with vascular smooth muscle cell proliferation and migration, Atherosclerosis 138 (1998) 79–89.

[21] A.C. Newby, A.B. Zaltsman, Molecular mechanisms in intimal hyperplasia, J. Pathol. 190 (2000) 300–309.

[22] A. Zalewski, Y. Shi, Vascular myofibroblasts. Lessons from coronary repair and remodeling, Arterioscler. Thromb. Vasc. Biol. 17 (1997) 417–422.

[23] K. Tanaka, M. Sata, Y. Hirata, R. Nagai, Diverse contribution of bone marrow cells to neointimal hyperplasia after mechanical vascular injuries, Circ. Res. 93 (2003) 783–790.

[24] Y. Xu, H. Arai, X. Zhuge, H. Sano, T. Murayama, M. Yoshimoto, T. Heike, T. Nakahata, S. Nishikawa, T. Kita, M. Yokode, Role of bone marrow-derived progenitor cells in cuff-induced vascular injury in mice, Arterioscler. Thromb. Vasc. Biol. 24 (2004) 477–482.

[25] M.R. Malinow, P.B. Duell, D.L. Hess, P.H. Anderson, W.D. Kruger, B.E. Phillipson, R.A. Gluckman, P.C. Block, B.M. Upson, Reduction of plasma homocyst(e)ine levels by breakfast cereal fortified with folic acid in patients with coronary heart disease, N. Engl. J. Med. 338 (1998) 1009–1015.

[26] N. Chacos, J. Capdevila, J.R. Falck, S. Manna, C. Martin-Wixtrom, S.S. Gill, B.D. Hammock, R.W. Estabrook, The reaction of arachidonic acid epoxides (epoxyeicosatrienoic acids) with a cytosolic epoxide hydrolase, Arch. Biochem. Biophys. 223 (1983) 639–648.

[27] X. Fang, T.L. Kaduce, N.L. Weintraub, M. VanRollins, A.A. Spector, Functional implications of a newly characterized pathway of 11,12-epoxyeicosatrienoic acid metabolism in arterial smooth muscle, Circ. Res. 79 (1996) 784–793.

[28] M. Rosolowsky, W.B. Campbell, Synthesis of hydroxyeicosatetraenoic (HETEs) and epoxyeicosatrienoic acids (EETs) by cultured bovine coronary artery endothelial cells, Biochim. Biophys. Acta 1299 (1996) 267–277.

[29] D.I. Axel, A. Frigge, J. Dittmann, H. Runge, I. Spyridopoulos, R. Riessen, R. Viebahn, K.R. Karsch, All-trans-retinoic acid regulates proliferation, migration, differentiation, and extracellular matrix turnover of human arterial smooth muscle cells, Cardiovasc. Res. 49 (2001) 851–862.

[30] K. Takeyabu, E. Yamaguchi, I. Suzuki, M. Nishimura, N. Hizawa, Y. Kamakami, Gene polymorphism for microsomal epoxide hydrolase and susceptibility to emphysema in a Japanese population, Eur. Respir. J. 15 (2000) 891–894.

[31] C.A. Smith, D.J. Harrison, Association between polymorphism in gene for microsomal epoxide hydrolase and susceptibility to emphysema, Lancet 350 (1997) 630–633.

[32] M. Sulkowska, S. Sulkowski, J. Dzieciol, Type II alveolar epithelial cells promote fibrosis during development of experimental lung emphysema, Folia Histochem. Cytobiol. 34 (Suppl. 1) (1996) 27–28.

[33] R.G. Thurman, F.C. Kauffman, Sublobular compartmentation of pharmacologic events (SCOPE): Metabolic fluxes in periportal and pericentral regions of the liver lobule, Hepatology 5 (1985) 144–151.

[34] T. Kietzmann, K. Jungermann, Modulation by oxygen of zonal gene expression in liver studied in primary rat hepatocyte cultures, Cell Biol. Toxicol. 13 (1997) 243–255.

Characterization of an exchangeable gene trap using pU-17 carrying a stop codon-*βgeo* cassette

Takuya Taniwaki,[1] Kyoko Haruna,[1,3] Hiroshi Nakamura,[1,3] Tomohisa Sekimoto,[1] Yuichi Oike,[1] Takashi Imaizumi,[1] Fumiyo Saito,[1] Mayumi Muta,[1] Yumi Soejima,[1,3] Ayako Utoh,[1,3] Naomi Nakagata,[2] Masatake Araki,[2] Ken-ichi Yamamura[1,3,*] and Kimi Araki[1,*]

[1]*Institute of Molecular Embryology and Genetics, Kumamoto University, Kuhonji 4-24-1, Kumamoto 862-0976, Japan,*
[2]*Institute of Resource Development and Analysis, Kumamoto University, Honjo 2-2-1, Kumamoto 860-0811, Japan, and*
[3]*TransGenic, 1155-5 Tabaru, Mashiki-machi, Kumamoto 861-2202, Japan*

We have developed a new exchangeable gene trap vector, pU-17, carrying the intron-*lox*71-splicing acceptor (SA)-*βgeo-lox*P-pA-*lox*2272-pSP73-*lox*511. The SA contains three stop codons in-frame with the ATG of *βgalactosidase/neomycin-resistance* fusion gene (*βgeo*) that can function in promoter trapping. We found that the trap vector was highly selective for integrations in the introns adjacent to the exon containing the start codon. Furthermore, by using the Cre-mutant *lox* system, we successfully replaced the *βgeo* gene with the *enhanced green fluorescent protein* (*EGFP*) gene, established mouse lines with the replaced clones, removed the selection marker gene by mating with Flp-deleter mice, and confirmed that the replaced *EGFP* gene was expressed in the same pattern as the *βgeo* gene. Thus, using this pU-17 trap vector, we can initially carry out random mutagenesis, and then convert it to a gain-of-function mutation by replacing the *βgeo* gene with any gene of interest to be expressed under the control of the trapped promoter through Cre-mediated recombination.

Key words: Cre/*lox*, embryonic stem cell, Flp/*FRT*, gene trap, site-specific recombination.

Introduction

The whole human and mouse genome sequences are now near to completion (Waterston *et al.* 2002). However, gene functions *in vivo* cannot be understood from the sequence information alone, and mutational analysis is a powerful and efficient approach for studying functional genomics. Gene trapping in embryonic stem (ES) cells is a proven method for isolating large numbers of random insertional mutations that can be easily identified (Gossler *et al.* 1989; Gossler 1993; Evans *et al.* 1997; Zambrowicz & Friedrich 1998; Stanford *et al.* 2001; Hansen *et al.* 2003; Stryke *et al.* 2003). Gene trap vectors contain a promoter-less reporter gene downstream of a splice acceptor (SA) and a selectable marker gene. When the gene trap vector is introduced and integrated into endogenous genes, a fusion transcript between the endogenous gene and the reporter gene is produced, such that the

*To whom correspondence should be addressed.
Email: arakimi@gpo.kumamoto-u.ac.jp,
yamamura@gpo.kumamoto-u.ac.jp

expression of the trapped gene can be monitored. Both the trapped cDNA and the genomic site of the integration can easily be cloned by rapid amplification of cDNA 5′-ends (5′-RACE) (Townley *et al.* 1997) and the plasmid rescue method (Araki *et al.* 1999). To date, trap vectors carrying the internal ribosomal entry site (IRES) from the encephalomyocarditis virus (ECMV) (Jang & Wimmer 1990; Ghattas *et al.* 1991; Mountford & Smith 1995; Kang *et al.* 1997) and the *βgalactosidase/neomycin-resistance* fusion gene (*βgeo*) (Friedrich & Soriano 1991; Voss *et al.* 1998) have been widely used and proven to trap various genes expressed in ES cells (Chowdhury *et al.* 1997; Bonaldo *et al.* 1998; Stoykova *et al.* 1998).

In typical gene trapping, insertion of a trap vector can only induce truncation mutations. In order to change the trapped alleles into a more subtle mutation, such as a point mutation, we previously developed a site-directed integration system in ES cells using the Cre-LE/RE mutant *lox* system (Araki *et al.* 1997), and constructed an exchangeable gene trap vector, pU-Hachi, carrying SA-*lox*71-IRES-*βgeo*–polyadenylation signal (pA)-*lox*P-pA-pUC (Araki *et al.* 1999). The *βgeo* gene in pU-Hachi trap clones can be replaced with any other cDNA of interest through Cre-mediated integration.

Therefore, we can carry out random insertional muta-genesis as the first step, and then introduce cDNA fragments for expression in the same pattern as the βgeo in the second step. Thus, we can also utilize trap clones as promoter resources.

However, there are several limitations to replacement experiments using pU-Hachi. First, the SA and *lox*71 sequences contain 4 and 1 stop codon(s), respectively. Hence, if a genomic gene carrying both exons and introns is inserted into the *lox*71 site, the stop codons present in the SA become premature transla-tion termination codons, leading to nonsense codon-mediated mRNA decay (NMD) (Wagner & Lykke-Andersen 2002). Second, because the IRES is used for cap-independent translation of the βgeo gene, it is necessary to use the IRES for translation of the inserted cDNA and this makes the construction of replacement vectors laborious. Third, trap vectors containing the IRES often integrate into the 3' region of a gene resulting in the production of a truncated form, which could modify the phenotype (Oike *et al.* 1999). Fourth, the 3'-part of the trapped gene cannot be reutilized, because the pA sequence is located outside the floxed region and cannot be removed. For example, we have tried 3'-rapid amplification of cDNA ends by inserting a promoter sequence, but no transcripts fused to the 3'-part of the trapped gene were produced. Fifth, it is difficult to insert and express the *cre* gene, because a re-excision reaction sometimes occurs in the LE/RE mutant *lox* system (Albert *et al.* 1995).

Recently, we showed that combination of the LE/RE mutant *lox* with a heterospecific *lox*, *lox*2272, improved the recombination efficiency and made it possible to integrate the *cre* gene through recombination by Cre (Araki *et al.* 2002). Based on these findings, we have constructed a new gene trap vector suitable for the insertion and expression of cDNA, genomic DNA and the *cre* gene. The new gene trap vector, pU-17, was designed to be a promoter trap and carried 3 kinds of mutant *lox* sites for replacement. We demonstrate here that pU-17 is efficiently integrated around the initiation codon, the βgeo gene is easily replaced with the enhanced green fluorescent protein (*EGFP*) gene, and the same expression pattern *in vivo* is maintained after the replacement.

Materials and Methods

Plasmids

The trap vectors pU-17 and pU-18 were constructed from the pU-Hachi vector by several modifications (Araki *et al.* 1999):

1. The *lox*71 site was inserted to the 5'-side, within the intron sequence of the mouse *En-2* gene.
2. The polyadenylation (pA) signal of the βgeo gene was removed.
3. A *lox*2272 sequence was inserted in front of the pA signal of the mouse *phosphoglycerate kinase-1* (*Pgk*) gene.
4. The pSP73 (Promega, Madison, WI, USA) vector was used instead of the pUC vector in pU-Hachi.
5. The IRES sequence was removed. The vectors were linearized at their single *Spe*I site before electroporation.

The Cre expression vector, pCAGGS-Cre, was described previously (Araki *et al.* 1995; Araki *et al.* 1997). The plasmid pCAGGS-Flp was constructed by ligating fragments of the *Flp* gene (Stratagene, La Jolla, CA, USA) into the *Eco*RI sites of pCAGGS. The mutation in the *Flp* gene (Ringrose *et al.* 1998) was corrected.

The replacement vector, p6SEFPPF, was assem-bled from components of pSP73 (Promega), the *lox* 66 sequence, the *EGFP* gene (Clontech, Palo Alto, CA, USA), the *FRT* sequence, the *Pgk* promoter, the *puromycin N-acetyltransferase* (*Pac*) gene and the *lox*P sequence.

Cell culture and electroporation

The ES cell lines TT2 (Yagi *et al.* 1993) and E14tg2a (Niwa *et al.* 2002) were grown as described. For electroporation with the pU-17 and pU-18 gene trap vectors, 80 μg of *Spe*I-digested DNA and 2×10^7 cells were used. The cells were suspended in 0.8 mL of phosphate-buffered saline (PBS), electroporated using a Bio-Rad Gene Pulser (Bio-Rad Laboratories, Hercules, CA, USA) set at 800 V and 3 μF, and then fed with medium supplemented with 200 μg/mL of G418 after 48 h. Selection was maintained for 7 days, and the colonies were then counted, picked and placed in 24-well plates. Replacement by Cre-mediated recombination in ES cells was performed as described previously (Araki *et al.* 1999).

Analyses of genomic DNA

Cells or tissues were lysed with sodium dodecylsul-fate (SDS)/proteinase K, treated with 1:1 (v/v) phenol/chloroform, precipitated with ethanol, and dissolved in 10 mM Tris-HCl, pH 7.5/1 mM ethylenediamine tetraacetic acid (EDTA) (TE). Six micrograms of genomic DNA was digested with appropriate restriction enzymes, electrophoresed in a 0.9% agarose gel and then blotted onto a nylon membrane

(Roche Diagnostics, Basel, Switzerland). Hybridization was performed using a DIG DNA Labeling Kit (Roche).

For polymerase chain reaction (PCR) analysis, DNA (50 ng) were subjected to 30 cycles of amplification (with each cycle consisting of 1 min at 94°C, 2 min at 55°C and 2 min at 72°C) in a thermal cycler. The primer sequences were as follows: for detection of the recombined allele, SA5 (5′-GGTCACTTTATGTTCTTGCCC-3′) and GFP2 (5′-TGTGATCGCCGTTCTCGTTG-3′); for detection of the *βgeo* sequence, Z1 (5′-GCGTTAC-CCAACTTAATCG-3′) and Z2 (5′-TGTGAGCGAGTAA-CAACC-3′); for detection of the *CAGGS-Flp* transgene, AG2 (5′-CTGCTAACCATGTTCATGCC-3′) and Flp5 (5′-ATCCTACCCCTTGCGCTAAA-3′).

RNA analyses

Total RNA was isolated from ES cells using Sepasol (Nakalai, Kyoto, Japan). Ten micrograms of total RNA was electrophoresed through 1.0% agarose-formaldehyde gels and transferred to a positively charged nylon membrane (Roche). After baking at 80°C for 1 h, the membrane was prehybridized, and then hybridized with RNA probes prepared using a DIG RNA Labeling and Detection Kit (Roche).

Five micrograms of total RNA was used for first-strand cDNA synthesis with the reverse transcriptase ReverScript (Wako Pure Chemical Industries, Osaka, Japan) and the LZUS3 primer (5′-GCGCATCGTAAC-CGTGCAT-3′) in the lacZ sequence. 5′-RACE was performed using the 5′-RACE system (Invitrogen, Carlsbad, CA, USA) according to the manufacturer's instructions. The initial PCR was performed using the primer SA13 (5′-TCTGAAACTCAGCCTTGAGC-3′) in the SA sequence and the anchor primer (5′-GGCCACGCGTCGACTAGTACGGGiiGGGiiGGGiiG-3′) (Invitrogen). Next, nested PCR was performed using the primer SA10 (5′-AGCAGTGAAGGCTGT-GCGA-3′) in the SA sequence and the amplification primer (5′-GGCCACGCGTCGACTAGTAC-3′) in the anchor primer sequence. The PCR product was electrophoresed, purified with Quantum Prep Freeze 'N Squeeze DNA Gel Extraction Spin Columns (Bio-Rad), and sequenced by the dideoxy-chain termination method using a Big Dye Terminator Cycle Sequencing kit (Perkin Elmer, Foster City, CA, USA). All the obtained sequences were confirmed by RT-PCR using first-strand cDNA synthesized with random primers. The obtained sequences were compared with the GenBank and GenEMBL databases using the BLASTN program (http://blast.genome.jp) (Altschul *et al.* 1990), and the exon-intron structures were examined using the Celera Discovery System (Applied Biosystems Japan, Tokyo, Japan).

Production of chimeric mice and microinjection

Chimeric mice were produced by aggregation of ES cells with eight-cell embryos of ICR mice (CLEA Japan, Tokyo, Japan). Chimeric male mice were mated with C57BL/6 J females (CLEA Japan) to obtain F1 heterozygotes.

For microinjection of CAGGS-Flp, superovulated BDF1 (Charles River, Osaka, Japan) females were mated with BDF1 males. Fertilized eggs were collected and pronuclear injection was performed according to a previously described procedure (Yamamura *et al.* 1984).

Histological analysis

For 5-bromo-4-chloro-3-indolyl β-D-galactopyranoside (X-gal) staining, tissues were fixed in 4% paraformaldehyde for 6 h, sectioned with a vibratome at 50 μm, treated with 1% Triton X-100 in PBS for 10 min, washed three times in PBS, incubated overnight at 30°C in staining solution (5 mM potassium ferricyanide, 5 mM potassium ferrocyanide, 2 mM $MgCl_2$, 0.5% X-gal in PBS), mounted on glass slides, and counterstained with Nuclear Fast red. For immunohistochemistry, paraffin sections were prepared and stained with an anti-EGFP rabbit polyclonal antibody (MBL, Nagoya, Japan).

Results

Construction of pU-17

The structure of pU-17 is shown in Figure 1(A). The improvements from pU-Hachi are as follows:

1. A *lox*71 site was inserted into the intron sequence of the SA.
2. *Lox2272* and *lox*511 sites were inserted into the downstream of the pA and plasmid vector tail, respectively. Through these two alterations, various replacements became possible (see Fig. 5 and Discussion).
3. The IRES was removed, and as a result, the three stop codons in the exon sequence of the SA were in-frame with the ATG of the *βgeo* gene (Fig. 1C). It is theoretically expected that only clones in which the vector is integrated into the upstream of the start codon of a trapped gene will become neo-resistant. Thus, this Stop-*βgeo* vector is expected to function in promoter trapping, and should be ideal for expressing cDNA under the control of a trapped gene. However, this restriction of the integration site may result in a reduction in the colony formation efficiency. Therefore, we examined the colony formation efficiency of pU-17 by comparison with a trap vector using the IRES of ECMV.
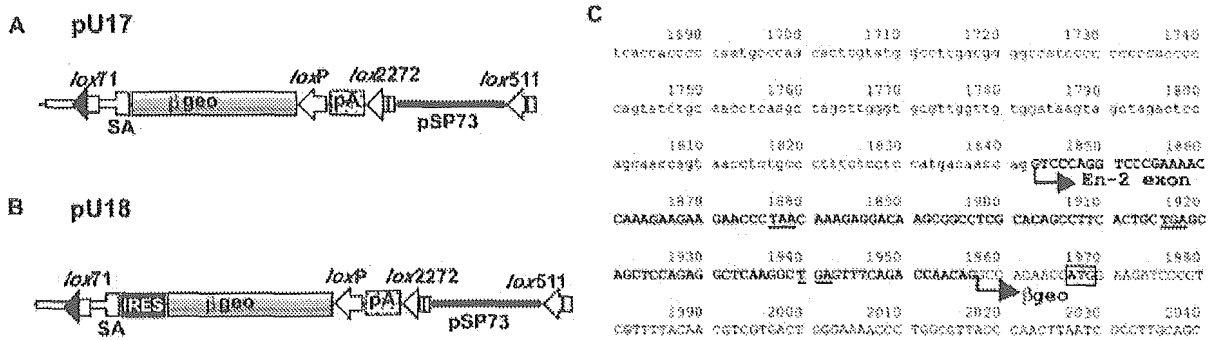
A   pU17

B   pU18

C

Fig. 1. Structure of the gene trap vectors. (a) Schematic representation of the trap vector pU-17. pU-17 contains 1.8 kb of an intron and a splice acceptor (SA) sequence from the mouse En-2 gene, the βgeo gene and a polyadenylation signal (pA). A lox71 site is located within the intron sequence, and loxP, lox2272 and lox511 sites are placed in the downstream of the βgeo, pA and pSP73 vector sequences, respectively. (b) Schematic representation of the trap vector pU-18. The only difference between pU-17 and pU-18 is the presence of the internal ribosomal entry site (IRES) sequence of encephalomyocarditis virus (ECMV) between the SA and βgeo. (c) Sequence of the junction of the SA and the βgeo gene of pU-17. Lower and upper case letters represent the intron and exon sequences, respectively. There are three in-frame stop codons (underlined) in the upstream of the βgeo initiation codon (boxed). It is theoretically expected that the integration site of the vector should be restricted to the upstream of the start codon of a trapped gene.

Table 1. Colony formation efficiencies of pU-17 and pU-18

Trap vector	Number of G418-resistant colonies		
	1st exp.	2nd exp.	3rd exp.
pU-17	34	135	36
pU-18	38	153	42

Eighty micrograms of linearized trap vector was introduced into 2×10^7 E14Tg2a cells. The electroporated cells were plated onto three 10 cm dishes and selected with G418 for 1 week, before the number of colonies was counted.

pU-17 has comparable colony formation efficiency to a trap vector containing an IRES

We constructed the pU-18 vector (Fig. 1B) carrying the IRES between the SA and βgeo. The only difference between pU-17 and pU-18 is the absence and presence of the IRES, respectively. In pU-18, a fusion message of the trapped gene and IRES-βgeo is produced, and translation starts from the AUG of both the trapped gene and βgeo. Therefore, trap clones should be G418-resistant independent of the insertion sites of the IRES-βgeo vector within the trapped genes (Bonaldo et al. 1998). The two vectors were introduced into ES cells harvested on the same day through electroporation. The cells were then selected with G418, and the numbers of colonies were counted. As shown in Table 1, almost the same numbers of colonies appeared with both vectors, indicating that the pU-17 Stop-βgeo vector has comparable colony formation efficiency to pU-18.

pU-17 integrates into the 5'-region of trapped genes

In order to examine the integration sites of pU-17 in trap clones, we first performed Northern blotting using randomly chosen pU-17 and pU-18 trap clones to compare the sizes of the fusion messages. If pU-17 integrates in the upstream of the start codon of a trapped gene, the lengths of trapped mRNA fused to βgeo should be short and therefore the total lengths of the fusion messages in pU-17 clones should be about 4.5 kb, corresponding to the length of SA-βgeo-pA. As shown in Figure 2(A), the sizes of the fusion messages in pU-17 clones were similar, spanning approximately 4.5–5 kb. On the other hand, various sizes of bands, most of which exceeded 5 kb, were detected in pU-18 clones, suggesting integration in the middle or 3'-half of the genes. This result indicates that pU-17 tends to integrate into the 5'-region of endogenous genes.

Next, to precisely analyze the insertion events in a larger number of trapped clones, trapped genes containing the pU-17 vector were determined by 5'-RACE analysis, and the results are summarized in Table 2. Regarding the 22 clones in which pU-17 was integrated into known genes, the integration sites in the context of their exon-intron structures were determined using the Celera Discovery System. As shown Figure 2(B), in 82% of the trap clones, pU-17 was integrated into the introns adjacent to the exon containing the start codon of the trapped gene. This results indicates that the pU-17 functions efficiently as a promoter trap vector.
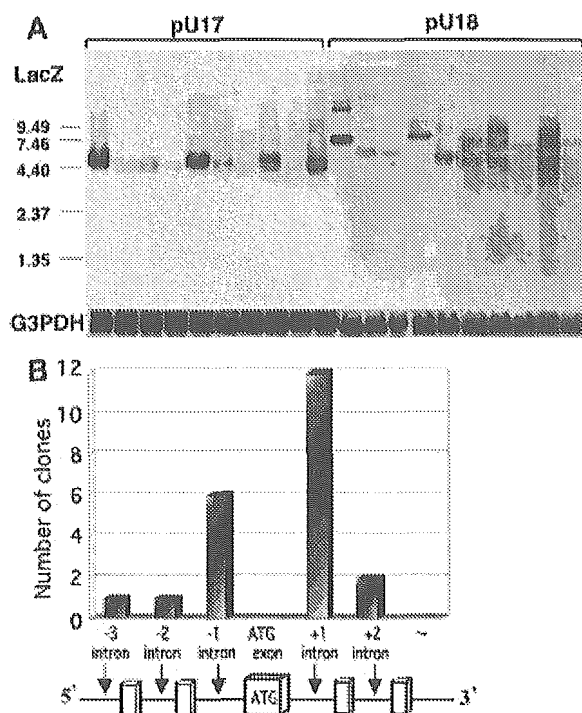
Fig. 2. (a) Northern blot analysis of trapped clones obtained using pU-17 (left) and pU-18 (right). RNA were prepared from embryonic stem (ES) clones carrying a single copy of the trap vector, and subjected to Northern blotting with a *LacZ* probe (upper) or *G3pdh* probe (lower). Size markers are shown on the left. (b) Histogram of the integration sites. Twenty-two clones in which a known gene was trapped were chosen, and the integration sites in the trapped genes were analyzed using the Celera Discovery System.

Table 2. Summary of the 5'-rapid amplification of cDNA ends (RACE) analysis results

Known	EST	Novel	ND[†]	Total
22 (17%)	61 (47%)	29 (22%)	17 (13%)	129 (100%)

The sequences obtained through 5'-RACE were compared to the published sequences in GenBank and the Celera Discovery System. †Not Determined: no product was obtained or part of the vector sequence (in many cases, the 5'-region of the intron sequence) was obtained.

Replacement of the βgeo gene with the EGFP gene

pU-17 carries four *lox* sites, such that the DNA sequence between *lox*71 and the other *lox* sites of *lox*P, *lox*2272 and *lox*511 can be replaced with another DNA sequence. To demonstrate the ability of pU-17 for such replacement, we performed targeted integration of the *EGFP* gene, as outlined in Figure 3. We constructed a replacement vector carrying a *lox*66-SA-*EGFP-FRT-Pgk* promoter-*Pac-FRT-*

*lox*P-pSP73. For the targeted replacement, 20 μg of each targeting plasmid and pCAGGS-Cre were electroporated into trap ES clones in their circular forms. Because the replacement vector and trap vector in the genome carry two *lox* sites with the same spacer region (*lox*66 and *lox*P, and *lox*71 and *lox*P, respectively), it is expected that intramolecular recombination should initially occur between the two *lox* sites after co-electroporation, resulting in the production of two intermediate molecules, as shown in the middle of Figure 3. Next, the ES cells in which targeted replacement has occurred were selected in the presence of puromycin. Because the *Pac* gene in the targeting vector does not have a pA signal, random integrants should be puromycin sensitive, and only upon Cre-mediated targeted integration, the *Pac* gene fuses to the pA signal on the trap vector, thereby making the cells drug-resistant. After removal of the *Pac* gene using the Flp/*FRT* system, the *EGFP* gene is expressed under the control of the trapped promoter. This removal is achieved by mating with *CAGGS-Flp* transgenic mice.

Two trap clones were used for the replacement experiment. The Ayu17–71 clone has trapped a novel gene and the expression pattern of the *βgeo* is ubiquitous (see Fig. 4). The Ayu17–104 clone has trapped the *Shroom* gene (Hildebrand & Soriano 1999) and shows a tissue-specific expression pattern.

After electroporation, 17 and 16 colonies from Ayu17–71 and Ayu17–104, respectively, were picked, expanded and analyzed for recombination events. To confirm the 5'- and 3'-junctions, we performed PCR and Southern blot hybridization with the Pac probe, respectively. Targeted insertion should give a 1.5 kb band in the PCR and a 2.4 kb band in the Southern blotting (Fig. 3A). Figure 3(B) shows the results for Ayu17–104 subclones, of which 15 of 16 clones (94%) revealed the pattern of targeted replacement. Ayu17–71 subclones also showed a high targeting frequency of 82% (Table 3). These results demonstrate that the replacement system using poly(A) trapping functions efficiently.

Germline transmission of the replaced clones and mating with CAGGS-Flp mice

We produced chimeric mice using two replaced clones derived from each of the parental Ayu17–71 and Ayu17–104 lines, and successfully obtained germline chimeras from all the subclones used. Next, the chimeric male mice were mated with *CAGGS-Flp* transgenic mice which express the *Flp* gene ubiquitously (data not shown). In the double-positive mice for the *CAGGS-Flp* transgene and the replaced trap vector,

recombination should occur between the *FRT* sites, resulting in deletion of the PGK-pac sequence. We confirmed the recombination using tail DNA from the double-transgenic mice and Southern blotting with the *EGFP* probe. The recombined allele gives a 1.4 kb band, whereas the original allele gives a 2.8 kb band. As shown in Figure 3, the expected 1.4 kb band was obtained in the all double-transgenic mice. However, only 40–80% of the progenies from the double-transgenic mice showed the recombined pattern (data not shown), indicating that the *Flp* gene is not expressed in all the germ cells in this *CAGGS-Flp* transgenic line.

Expression pattern of the integrated EGFP gene

The *in vivo* expression pattern of the targeted integrated *EGFP* gene should be identical to that of the *βgeo* gene expression in the parental lines. First, we

Fig. 3. Replacement of *βgeo* with *enhanced green fluorescent protein* (*EGFP*) and removal of the marker gene using the Flp/ FRT system. (a) Scheme of the gene replacement. The structures of the integrated trap vector and targeting vector plasmid are shown in the top panel. The targeting vector p6SEFPPF carries *lox*66-SA-*EGFP-FRT-Pgk* promoter-*Pac-FRT-lox*P-pSP73. p6SEFPPF and the Cre-expression vector, pCAGGS-Cre, are co-electroporated into trap ES cells, and targeted recombinant cells are selected with puromycin. The expected intermediates produced through intermolecular recombination are shown in the second panel, followed by the allele replaced with the *EGFP* gene through Cre-mediated recombination. After establishment of a mouse line from the replaced clone, the selectable marker gene, *Pgk-Pac*, is removed by Flp/*FRT* recombination through mating with *CAGGS-Flp* transgenic mice. The recombined allele by Flp recombinase is shown in the bottom panel. The positions of the primers SA5 and GFP2, and the EGFP and Pac probes used for the Southern blotting are indicated by arrows and solid bars labeled 'probe', respectively. The expected sizes of the polymerase chain reaction (PCR) products and signals in Southern blotting are also indicated. E, *Eco*RI; EV, *Eco*RV; B, *Bam*HI; P, *Pst*I. (b) PCR and Southern blot analysis to detect targeted integration of the SA-*EGFP-FRT-Pgk-Pac-FRT* unit in subclones of Ayu17–104. Genomic DNA from 16 randomly picked subclones were subjected to PCR with SA5 and GFP2 to detect their 5′-junctions. For detection of their 3′-junctions, the genomic DNA were digested with *Eco*RV and *Eco*RI and hybridized with the Pac probe. Fifteen of 16 clones showed the expected pattern of targeted replacement, namely 1.5 kb in PCR and 2.4 kb in Southern blotting. The E + B lane represents *Eco*RI and *Bam*HI digestion, which should give 2.3 kb regardless of the integration position. (c) Detection of recombination by Flp recombinase. Genomic tail DNA of F1 offspring obtained from mating of chimeric male mice and *CAGGS-Flp* female transgenic mice were prepared and examined for the existence of the replaced allele and the *CAGGS-Flp* transgene by PCR. The PCR results are indicated at the top by a plus or minus. Next, the DNA were digested by *Pst*I and hybridized with the *EGFP* probe to detect
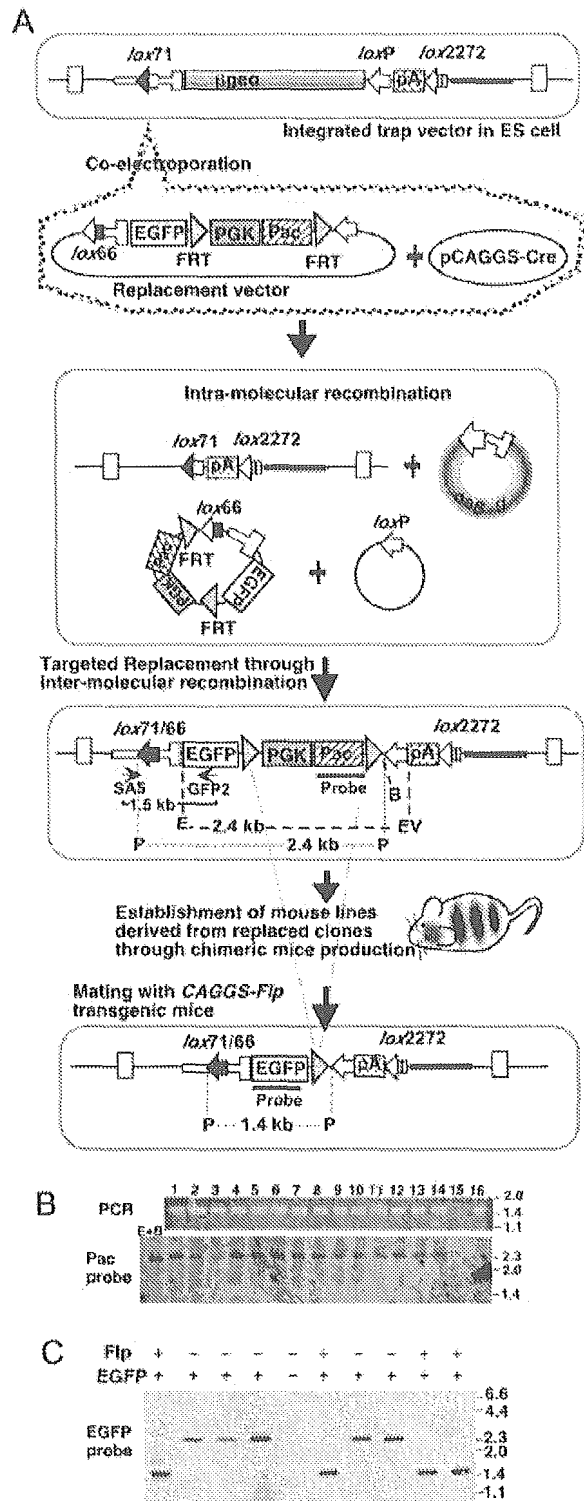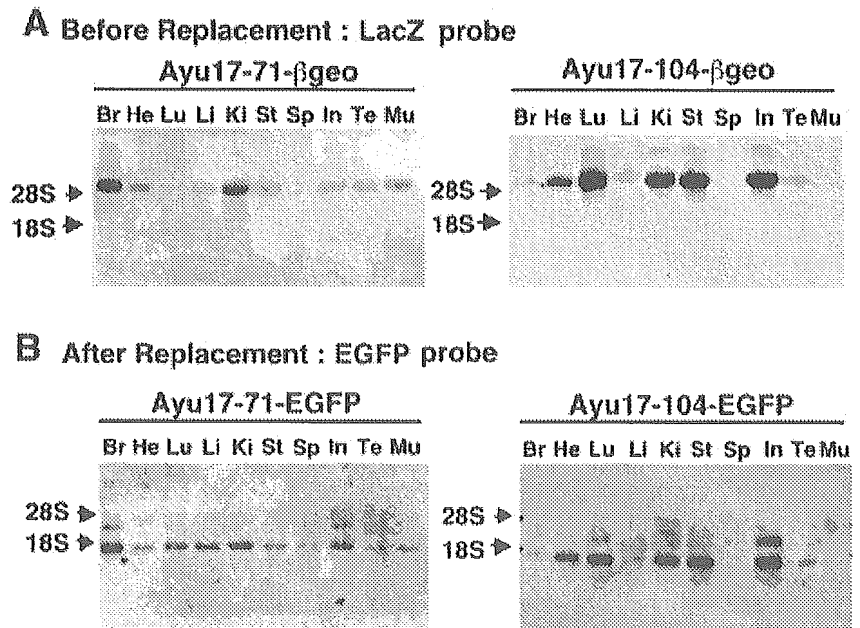
recombination between FRT sites. Recombined alleles should give a 1.4 kb band, whereas unrecombined alleles should produce a 2.8 kb band. In all the double-transgenic mice, a 1.4 kb band is detected, indicating deletion of the PGK-Pac sequence through recombination by Flp.

Table 3. Results of targeted replacement with the *EGFP* gene

Parental cell line	Total no. of colonies	No. of colonies analyzed	No. of colonies with targeted integration	% of targeted integration
Ayu17–71	22	17	14	82
Ayu17–104	109	16	15	94

Fig. 4. Expressions of the *βgeo* and *EGFP* genes. (A) Northern blot analysis with the *LacZ* probe. Total RNA were extracted from tissues of adult hemizygous *Ayu17–71-βgeo* or *Ayu17–104-βgeo* trap mice, that had been established from parental trap clones carrying the *βgeo* gene, and subjected to Northern blotting. (B) Northern blot analysis with the *EGFP* probe. Double-positive F1 mice of the trap allele replaced with the *EGFP* gene and the *CAGGS-Flp* transgene were used. Br, brain; He, heart; Lu, lung; Li, liver; Ki, kidney; St, stomach; Sp, spleen; In, intestine; Te, testis; Mu, muscle.

A Before Replacement : LacZ probe

Ayu17-71-βgeo   Ayu17-104-βgeo

Br He Lu Li Ki St Sp In Te Mu   Br He Lu Li Ki St Sp In Te Mu

28S ▶   28S ▶
18S ▶   18S ▶

B After Replacement : EGFP probe

Ayu17-71-EGFP   Ayu17-104-EGFP

Br He Lu Li Ki St Sp In Te Mu   Br He Lu Li Ki St Sp In Te Mu

28S ▶   28S ▶
18S ▶   18S ▶

examined the expression pattern by Northern blotting. Figure 4(A) shows the *βgeo* expression in heterozygous mice established from the parental trap lines before replacement, and Figure 4(B) shows the *EGFP* expression in double-positive F1 mice for the replaced trap allele and the *CAGGS-Flp* transgene. In the *Ayu17–71* line, *βgeo* expression was ubiquitous, but the brain and kidneys showed stronger expression. After replacement, the same expression pattern was observed for the *EGFP* gene. In the *Ayu17–104* line, *βgeo* expression was detected in the heart, lungs, kidneys, stomach and intestine, and the integrated *EGFP* gene showed the same expression pattern. In several tissues, extra bands of about 2.4 kb were detected. This size was identical to the size observed in the single-positive *EGFP* mice before recombination by Flp (data not shown), indicating that the recombination by Flp was not complete.

Next, we further confirmed the expression pattern at the cellular level by histological analysis with X-gal staining in the parental *βgeo* lines and immunostaining with an anti-EGFP antibody in the replaced *EGFP* lines. As shown in Figure 5, positive signals in the Purkinje cells, cerebrum and renal medulla in the

Ayu17–71 line (Fig. 5A) and the mucosa of the stomach and the glomerulus of the kidney in the *Ayu17–104* line (Fig. 5B) were detected in both staining procedures. Thus, the inserted *EGFP* gene was expressed with the same cell-type specific pattern as the original *βgeo* gene.

Discussion

Here, we have demonstrated that our exchangeable promoter trap system functioned as expected, in that the trap vector was selectively inserted into the 5′-region of endogenous genes, the *βgeo* reporter gene was easily replaced with another gene and, importantly, the inserted gene was expressed in the same pattern as the *βgeo* gene *in vivo*.

In addition to replacement of the reporter gene, many other replacements can be performed using the pU-17 trap clones, as shown in Figure 6. First, any genomic DNA or cDNA of interest can be expressed through replacement between *lox*71 and *lox*P (Fig. 6A). We can also introduce any type of mutation, such as a point or dominant-negative mutation. Second, through replacement between *lox*71 and *lox*2272, the *cre* gene can also be inserted and
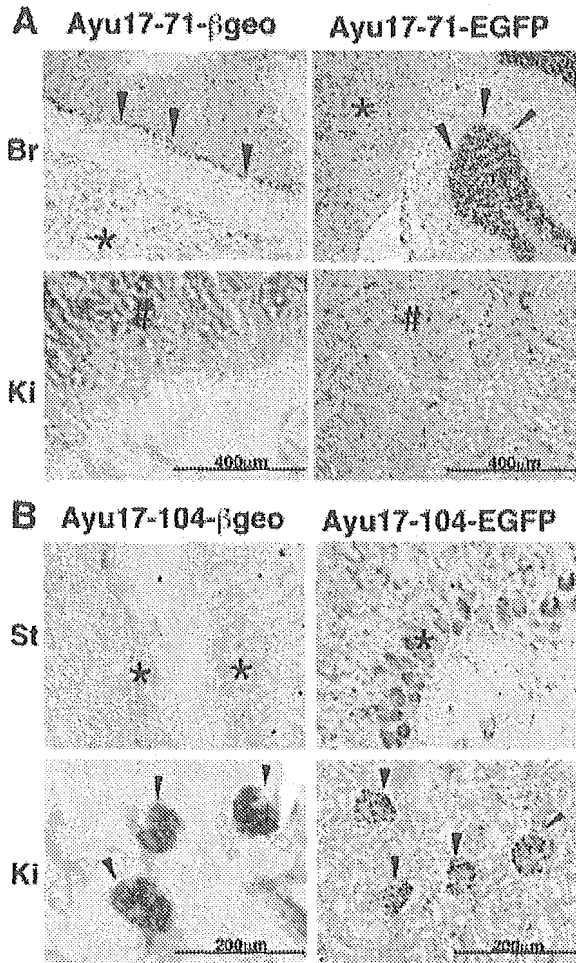
A   Ayu17-71-βgeo   Ayu17-71-EGFP

Br

Ki

B   Ayu17-104-βgeo   Ayu17-104-EGFP

St

Ki

Fig. 5. Histological analysis of the expressions of the *βgeo* and *EGFP* genes. (a) The brain (Br) and kidney (Ki) from original *Ayu17-71-βgeo* and replaced *Ayu17-71-EGFP* mice were stained with X-gal (left) and an anti-EGFP antibody (right), respectively. In both staining procedures, positive signals are detected in the Purkinje cells (arrow heads), cerebrum (*) and renal medulla (#). (b) The stomach (St) and kidney (Ki) from original *Ayu17-104-βgeo* and replaced *Ayu17-104-EGFP* mice were stained with X-gal (left) and an anti-EGFP antibody (right), respectively. In both staining procedures, positive signals are detected in the mucosa of the stomach (*) and glomerulus of the kidney (arrow heads).

Fig. 6. Replacement patterns in trap clones with pU-17. (a) Replacement between *lox*71 and *lox*P. Any cDNA (upper) or genomic DNA (lower) of interest can be inserted and expressed under the control of the trapped promoter activity. (b) Replacement between *lox*71 and *lox*2272. The *cre* gene can also be expressed under the control of the trapped promoter activity (upper). If a promoter sequence followed by a splice donor site (SD) is inserted, it is possible to change the expression pattern of the trapped gene.

expressed (Fig. 6B, upper) as described previously (Araki *et al.* 2002). Because we can choose trap lines with the desired expression pattern by observing the *βgeo* expression, this should be convenient for the production of various Cre-mice. Third, in cases of integration of the trap vector into the 5′-region of the endogenous ATG, we can alter the expression pattern of the trapped gene by inserting an exogenous promoter (Fig. 6B, lower). By using a strong promoter in ES cells, this would be useful for 3′-RACE to deter-
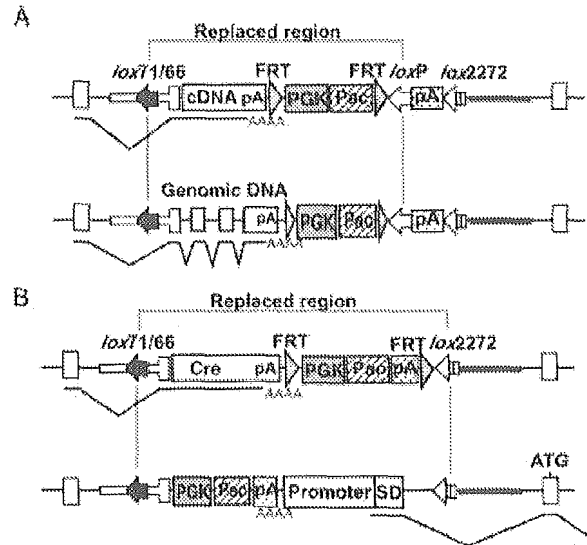
mine the trapped gene when 5′-RACE fails or only produces quite a short sequence. In all cases, the selection marker gene used for replacement can be removed through mating with *CAGGS-Flp* mice.

In the pU-17 vector, we inserted in-frame stop codons in the upstream of the ATG of the *βgeo* gene for the convenience being able to express the inserted cDNA after replacement. It is not necessary to use the IRES or adjust the reading frames between the trapped gene and the inserted cDNA for this expression. Theoretically, this should reduce the colony formation efficiency, but our results revealed no significant differences in the colony formation efficiencies between vectors with and without IRES. We confirmed that the vector integration sites in pU-18 clones were completely random (data not shown), indicating that the IRES in pU-18 functioned as expected in the trap clones. We suppose that IRES-dependent translation is affected by the surrounding sequence and cannot always start efficiently. On the other hand, Bonaldo *et al.* (1998) reported that their SA-IRES-*βgeo* vector showed 6.7-fold higher colony formation efficiency than their SA-*βgeo* vector. Although the reason for this result is not clear, it would be due to the absence of the start codon of the *βgeo* in their SA-*βgeo* vector. With their vector,

therefore, trap clones become G418 resistant only when a stable and active fusion protein of the βgeo and trapped gene is produced from the trapped allele. We speculate that the probability of the production of active fusion protein would be much lower than that of successful trap event with pU-17.

The trap vector pU-17 showed a strong bias to integration into the 5'-region of the genes. It is well known that retroviral vectors show a tendency for integration into the 5'-end of genes (Friedrich & Soriano 1991; von Melchner *et al.* 1992), but no plasmid trap vectors have been reported to have such a tendency, except for pKC199βgeo, reported by Thomas *et al.* (2000). The vector pKC199βgeo also has an in-frame stop codon with the ATG of the βgeo, although they did not describe it but discussed other four possible reasons for the tendency to integrate into the 5'-end of genes. Thus, the structure of the SA carrying in-frame stop codon with the start codon of the βgeo would be useful for enriching integration near the 5' end of genes.

In 64% of the trap clones, pU-17 vector was integrated into the downstream of the exon containing the start codon of the trapped gene (Fig. 2B). It is known that upstream AUG codons and open reading frames (uAUG/uORF) are common features of mRNA for mainly negative control of translation from the main AUG (Morris & Geballe 2000; Kozak 2002), and it is estimated that about half of human mRNA have uAUG/uORF (Suzuki *et al.* 2000). Leaky scanning and reinitiation mechanisms of ribosomes enable the downstream main AUG codons to be accessed by translation machinery (Kozak 2002). Although uAUG/uORF diminish translation of the main ORF, it is reported that approximately 40% of ribosomes were able to initiate twice and approximately 25% were able to initiate three times (Wang & Rothnagel 2004). Because the ORF started from endogenous AUG should act as uORF in 'downstream-integrated' trap clones, it is considered that the translation initiation of the βgeo would be somewhat lower level than that of the endogenous trapped gene, but enough for acquirement of G418 resistance. Whether the βgal activity in 'downstream-integrated' trap mice exactly reflect the expression pattern of the trapped genes or not can be easily tested by targeted insertion of the IRES-LacZ construct, and this analysis is now in progress.

We have performed targeted integration with more than 20 exchangeable trap clones, and in all clones except for one (Araki *et al.* 1999), we successfully obtained recombined clones at high frequencies of 80–95%. Thus, the targeted integration is highly reproducible. Our exchangeable gene trap system can overcome the limitations of conventional gene trapping and will be an ideal means for large-scale mutagenesis.

References

Albert, H., Dale, E. C., Lee, E. & Ow, D. W. 1995. Site-specific integration of DNA into wild-type and mutant *lox* sites placed in the plant genome. *Plant J.* **7**, 649–659.

Altschul, S. F., Gish, W., Miller, W., Myers, E. W. & Lipman, D. J. 1990. Basic local alignment search tool. *J. Mol. Biol.* **215**, 403–410.

Araki, K., Araki, M., Miyazaki, J. & Vassalli, P. 1995. Site-specific recombination of a transgene in fertilized eggs by transient expression of Cre recombinase. *Proc. Natl Acad. Sci. USA* **92**, 160–164.

Araki, K., Araki, M. & Yamamura, K. 1997. Targeted integration of DNA using mutant lox sites in embryonic stem cells. *Nucleic Acids Res.* **25**, 868–872.

Araki, K., Araki, M. & Yamamura, K. 2002. Site-directed integration of the cre gene mediated by Cre recombinase using a combination of mutant *lox* sites. *Nucleic Acids Res.* **30**, e103.

Araki, K., Imaizumi, T., Okuyama, K., Oike, Y. & Yamamura, K. 1997. Efficiency of recombination by Cre transient expression in embryonic stem cells: comparison of various promoters. *J. Biochem. (Tokyo)* **122**, 977–982.

Araki, K., Imaizumi, T., Sekimoto, T. *et al.* 1999. Exchangeable gene trap using the Cre/mutated *lox* system. *Cell Mol. Biol. (Noisy-le-Grand)* **45**, 737–750.

Bonaldo, P., Chowdhury, K., Stoykova, A., Torres, M. & Gruss, P. 1998. Efficient gene trap screening for novel developmental genes using IRES βgeo vector and in vitro preselection. *Exp. Cell Res.* **244**, 125–136.

Chowdhury, K., Bonaldo, P., Torres, M., Stoykova, A. & Gruss, P. 1997. Evidence for the stochastic integration of gene trap vectors into the mouse germline. *Nucleic Acids Res.* **25**, 1531–1536.

Evans, M. J., Carlton, M. B. L. & Russ, A. P. 1997. Gene trapping and functional genomics. *Trends Genet* **13**, 370–374.

Friedrich, G. & Soriano, P. 1991. Promoter traps in embryonic stem cells: a genetic screen to identify and mutate developmental genes in mice. *Genes Dev.* **5**, 1513–1523.

Ghattas, I. R., Sanes, J. R. & Majors, J. E. 1991. The encephalomyocarditis virus internal ribosome entry site allows efficient coexpression of two genes from a recombinant provirus in cultured cells and in embryos. *Mol. Cell Biol.* **11**, 5848–5859.

Gossler, A. & Zachgo, J. 1993. Gene and enhancer trap screens in ES cell chimeras. *Gene Targeting: a Practical Approach.* (ed. Joyner A.) pp. 181–227. Oxford University Press, Oxford.

Gossler, A., Joyner, A. L., Rossant, J. & Skarnes, W. C. 1989. Mouse embryonic stem cells and reporter constructs to detect developmentally regulated genes. *Science* **244**, 463–465.

Hansen, J., Floss, T., Van Sloun, P. *et al.* 2003. A large-scale, gene-driven mutagenesis approach for the functional analysis of the mouse genome. *Proc. Natl Acad. Sci. USA* **100**, 9918–9922.

Hildebrand, J. D. & Soriano, P. 1999. Shroom, a PDZ. domain-containing actin-binding protein, is required for neural tube morphogenesis in mice. *Cell* **99**, 485–497.

Jang, S. K. & Wimmer, E. 1990. Cap-independent translation of encephalomyocarditis virus RNA: structural elements of the internal ribosomal entry site and involvement of a cellular 57-kD RNA-binding protein. *Genes Dev.* **4**, 1560–1572.

Kang, H. M., Kang, N. G., Kim, D. G. & Shin, H. S. 1997. Dicistronic tagging of genes active in embryonic stem cells of mice. *Mol. Cells* **7**, 502–508.

Kozak, M. 2002. Pushing the limits of the scanning mechanism for initiation of translation. *Gene* **299**, 1–34.

von Melchner, H., DeGregori, J. V., Rayburn, H., Reddy, S., Friedel, C. & Ruley, H. E. 1992. Selective disruption of genes expressed in totipotent embryonal stem cells. *Genes Dev.* **6**, 919–927.

Morris, D. R. & Geballe, A. P. 2000. Upstream open reading frames as regulators of mRNA translation. *Mol. Cell Biol.* **20**, 8635–8642.

Mountford, P. S. & Smith, A. G. 1995. Internal ribosome entry sites and dicistronic RNAs in mammalian transgenesis. *Trends Genet* **11**, 179–184.

Niwa, H., Masui, S., Chambers, I., Smith, A. G. & Miyazaki, J. 2002. Phenotypic complementation establishes requirements for specific POU domain and generic transactivation function of Oct – 3/4 in embryonic stem cells. *Mol. Cell Biol.* **22**, 1526–1536.

Oike, Y., Hata, A., Mamiya, T. *et al.* 1999. Truncated CBP protein leads to classical Rubinstein–Taybi syndrome phenotypes in mice: implications for a dominant-negative mechanism. *Hum. Mol. Genet* **8**, 387–396.

Ringrose, L., Lounnas, V., Ehrlich, L. *et al.* 1998. Comparative kinetic analysis of FLP and cre recombinases: mathematical models for DNA binding and recombination. *J. Mol. Biol.* **284**, 363–384.

Stanford, W. L., Cohn, J. B. & Cordes, S. P. 2001. Gene-trap mutagenesis: past, present and beyond. *Nat. Rev. Genet* **2**, 756–768.

Stoykova, A., Chowdhury, K., Bonaldo, P. *et al.* 1998. Gene trap expression and mutational analysis for genes involved in the development of the mammalian nervous system. *Dev. Dyn.* **212**, 198–213.

Stryke, D., Kawamoto, M., Huang, C. C. *et al.* 2003. BayGenomics: a resource of insertional mutations in mouse embryonic stem cells. *Nucleic Acids Res.* **31**, 278–281.

Suzuki, Y., Ishihara, D., Sasaki, M. *et al.* 2000. Statistical analysis of the 5′ untranslated region of human mRNA using 'Oligo-Capped' cDNA libraries. *Genomics* **64**, 286–297.

Thomas, T., Voss, A. K., Chowdhury, K. & Gruss, P. 2000. A new gene trap construct enriching for insertion events near the 5′ end of genes. *Transgenic Res.* **9**, 395–404.

Townley, D. J., Avery, B. J., Rosen, B. & Skarnes, W. C. 1997. Rapid sequence analysis of gene trap integrations to generate a resource of insertional mutations in mice. *Genome Res.* **7**, 293–298.

Voss, A. K., Thomas, T. & Gruss, P. 1998. Efficiency assessment of the gene trap approach. *Dev. Dyn.* **212**, 171–180.

Wagner, E. & Lykke-Andersen, J. 2002. mRNA surveillance: the perfect persist. *J. Cell Sci.* **115**, 3033–3038.

Wang, X. Q. & Rothnagel, J. A. 2004. 5′-untranslated regions with multiple upstream AUG codons can support low-level translation via leaky scanning and reinitiation. *Nucleic Acids Res.* **32**, 1382–1391.

Waterston, R. H., Lindblad-Toh, K., Birney, E. *et al.* 2002. Initial sequencing and comparative analysis of the mouse genome. *Nature* **420**, 520–562.

Yagi, T., Tokunaga, T., Furuta, Y. *et al.* 1993. A novel ES cell line, TT2, with high germline-differentiating potency. *Anal Biochem.* **214**, 70–76.

Yamamura, K., Kikutani, H., Takahashi, N. *et al.* 1984. Introduction of human γ1 immunoglobulin genes into fertilized mouse eggs. *J. Biochem. (Tokyo)* **96**, 357–363.

Zambrowicz, B. P. & Friedrich, G. A. 1998. Comprehensive mammalian genetics: history and future prospects of gene trapping in the mouse. *Int. J. Dev. Biol.* **42**, 1025–1036.